Rochester Institute of Technology
RIT Digital Institutional Repository

Theses

7-2020

Effect of Laser Texturing and Varying Dimple Density on Tribological Properties of Titanium-Ceramic Contact

Akshay Gaikwad
agg7834@rit.edu

Follow this and additional works at: https://repository.rit.edu/theses

Recommended Citation
Gaikwad, Akshay, "Effect of Laser Texturing and Varying Dimple Density on Tribological Properties of Titanium-Ceramic Contact" (2020). Thesis. Rochester Institute of Technology. Accessed from

This Thesis is brought to you for free and open access by the RIT Libraries. For more information, please contact repository@rit.edu.

RIT

Effect of Laser Texturing and Varying Dimple Density on Tribological Properties of Titanium-Ceramic Contact

Submitted by,

Akshay Gaikwad

A Thesis Submitted in Partial Fulfillment of the Requirement for Master of Science in Mechanical Engineering

Department of Mechanical Engineering

Kate Gleason College of Engineering

Rochester Institute of Technology

Rochester, NY

July 2020

Committee Approval:

Dr. Patricia Iglesias Victoria **Date:**

Thesis Advisor.
Department of Mechanical Engineering

Dr. Michael Schertzer **Date:**

Committee Member
Department of Mechanical Engineering

Dr. Rui Liu **Date:**

Committee Member
Department of Mechanical Engineering

Dr. Michael Schrlau **Date:**

Department Representative
Department of Mechanical Engineering

ABSTRACT

The loss of energy due to friction is one of the major problems industries are facing nowadays. Friction reduces the mechanical efficiency of the machine components. It is estimated that an average of 40% energy is lost to overcome the friction. In recent years, surface modification and surface texturing have shown tremendous ability to reduce friction and wear. Microstructures generated on the surface act as a secondary reservoir for lubricants and wear particle receptacles to reduce further abrasion. In addition, surface texturing boost hydrodynamic pressure which increases the *elasto-hydrodynamic lubrication regime* of the *Stribeck* curve, reducing friction and wear. There are different techniques used to texture the surfaces such as sandblasting, acid etching, laser texturing, modulation-assisted machining, etc. Amongst all these techniques, laser texturing is the most popular due to its advantages like high accuracy, good consistency and celerity as compared to other techniques. This study focuses on the effects of laser texturing on tribological properties of titanium alloy Ti6Al4V when in contact with a tungsten carbide ball. The effect of varying the dimple density on friction is studied using PAO as a lubricant in titanium-tungsten carbide contact. Tests were performed on 8 samples with different dimple densities and on an untextured sample. These different dimple densities were achieved by using different laser speeds. Increasing in the laser speed results in a decrease in the dimple density. Results showed that friction, as well as wear, is reduced for all the textured samples as compared to an untextured sample. For the two samples with the highest dimple densities and laser speeds of 400mm/s and 800mm/s, friction is reduced by 67% as compared to untextured surface. However, for the sample with laser speed of 400mm/s and dimple density of 50dimples/mm the surface

hardness is increased considerably due to a longer exposure to laser, which can affect the tribological properties of the material. The second sample with laser speed of 800mm/s and dimple density of 25dimples/mm shows very low increase in surface hardness and it can be said that the reduction in friction is the effect of laser texturing. For other samples with intermediate dimple densities and laser speeds from 1200mm/s to 2800mm/s, the friction coefficient stays low until the dimples wear out from the surface and then increases to a value similar to the friction coefficient of untextured surface. Overall, the texturing of the metal surface improves tribological properties of the metal.

ACKNOWLEDGEMENT

I would like to thank Dr. Patricia Iglesias Victoria for giving me this great opportunity and believing in me. I couldn't have achieved this without her support and valuable guidance. Her trust and confidence in me always pushed me to be the best version of myself throughout this wonderful journey.

I would also like to thank my thesis committee members Dr. Michael Schertzer, Dr. Rui Liu and Dr. Michael Schrlau for evaluating my work. I would also like to thank my fellow lab-mates Hong Guo, Sameer Magar, Paarth Mehta and Irene Del Sol for all your support and good times in the lab.

Finally, I would also like to thank my parents, without them I am as good as nothing.

TABLE OF CONTENTS

LIST OF FIGURES

LIST OF TABLES

NOMENCLATURE

EJ – Exajoule

$MtCO_2$ – Metric tons of CO_2

RPM – revolutions per minute

Pa – Pascal

Pas – Pascal second

mm – millimeter

Hz – Hertz

N - Newton

ABBREVIATIONS

BL – Boundary Lubrication

ML – Mixed Lubrication

EHL – *Elasto-Hydrodynamic* Lubrication

PAO – Polyalphaolefin

TC – Tungsten - Carbide

1.0 PROBLEM INTRODUCTION

Almost all industries in the world have mechanical components with relative motion between each other. This relative motion causes friction between mating components. A large amount of energy is lost to overcome the friction in machine components. In the transportation industry, friction consumes almost 60% of the energy produced [1]. Globally, energy consumed due to friction and wear is around 103 EJ and 16 EJ respectively. The cost incorporated to overcome this friction is estimated to be 285,500 million US Dollars [1].

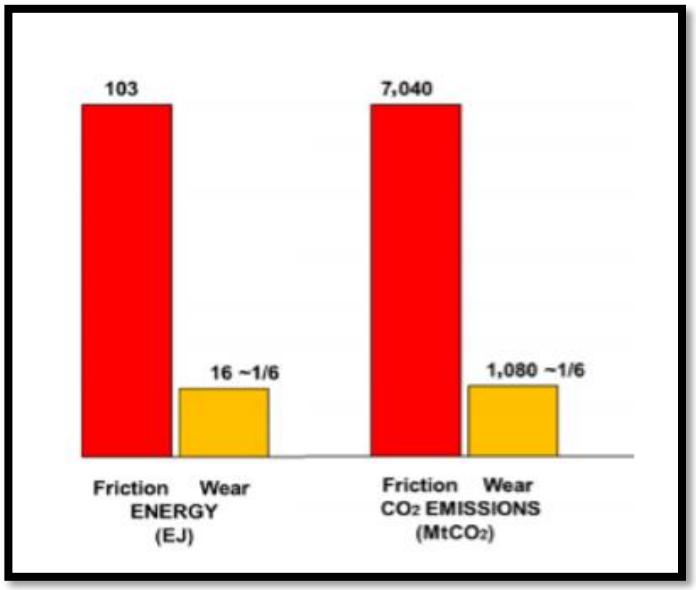

Figure 1: Energy consumption and CO2 emission due to friction and wear globally [1].

In this 21st century, due to the emission of greenhouse gasses, world is facing a global warming issue. CO_2 is the main contributor to greenhouse gasses. Friction and wear indirectly emits around 7040 $MtCO_2$ and 1080 $MtCO_2$ of CO_2 globally every year [1].

Wang et al. [2] showed that surface texturing can help reducing energy consumption and emission of CO_2 gasses. Textured surfaces improve wettability and lubrication property of metals. As a result, in vehicles, power output, emission, and fuel consumption are improved. There are different methods which are used to texture the surfaces. These methods include sandblasting, acid etching, media blasting, modulation-assisted machining, electron-beam, ion-beam laser texturing.

Each of the above techniques has its own advantages and disadvantages, but the laser texturing method is the most effective because of its unique advantages over other methods. Laser texturing method provides high precision with a wide range of dimple size and shapes. As there is no waste generated in laser texturing it is an environmentally friendly method. It is also easy to control the dimple density and dimple depth by just varying the laser parameters [3].

In this thesis, the friction and wear behavior of textured samples generated using the laser texturing method will be studied. The effect of the varying dimple density on tribological properties will also be examined.

2.0 THE RESEARCH QUESTION

Numerous studies have shown that surface texturing improves the tribological properties of components in contact in mechanical applications. Over the years, several techniques have been developed. This thesis will study the textured surfaces generated by laser texturing. The research questions that must be answered are:

- Will textured surfaces created by laser texturing improve the tribological properties of titanium?
- How changing the laser speed will affect the dimple density of textured surface?
- How varying dimple density on the textured surface affects the tribological properties of metal in contact?
- What optimum dimple density will provide maximum improvement in the tribological properties of titanium?

3.0 LITERATURE REVIEW

3.1 Tribology

Friction is a resisting force which impedes the relative motion in solid surfaces, fluid layers, and any other sliding surfaces. Friction is important and desirable for supplying traction in our day to day activities such as walking, braking a car or changing the direction. A sudden reduction in traction in these cases can cause loss of control and accidents. However, it is necessary to make sure that its effects are minimized in machine applications like bearings, piston, and cylinder, gears, etc, to save energy. This reduction in friction can be achieved by the use of lubricant between two contacting surfaces [4].

Two surfaces in moving contact experience friction. This relative motion between surface causes erosion and removes material from surfaces. This material removal is called wear [5]. To reduce friction and wear of the materials we need to study the tribological properties of materials under certain applications.

Tribology is the study of friction, lubrication and wear. Tribology can be defined as the science and technology of interacting surfaces in relative motion. The word “tribology” derives from the Greek root of the verb ‘tribo’ which means ‘rubbing’ and the suffix ‘logy’ means ‘study of’. In 1966 Peter Jost first coined the word tribology. Though tribology research can range from macro to nano scales, it is traditionally concentrated on transport and manufacturing sectors [6].

3.2 Stribeck Curve

In 1902, Richard *Stribeck* studied the friction coefficient properties in bearings. He plotted a graph of friction coefficient against the bearing number which is also known as Hersey number. This curve between the coefficient of friction and a Hersey number is called a *Stribeck* curve [6]. The Hersey number is the dimensionless number obtained from the sliding velocity (m/s) times the dynamic viscosity (N·s/m^2), divided by the load per unit length of bearing (N/m). The formula for Hersey number is shown in equation 1 below:

$$\text{Hersey Number} = \eta * \frac{V}{P} \qquad \text{Equation 1}$$

Where, η is dynamic viscosity in N·s/m^2,

V is sliding velocity in m/s, and

P is load per unit length in N/m.

Here, sliding velocity is the relative velocity between two mating surfaces and a unit load is applied load over a projected area. When we plot *Stribeck* curve, we get different domains of lubrication [7].

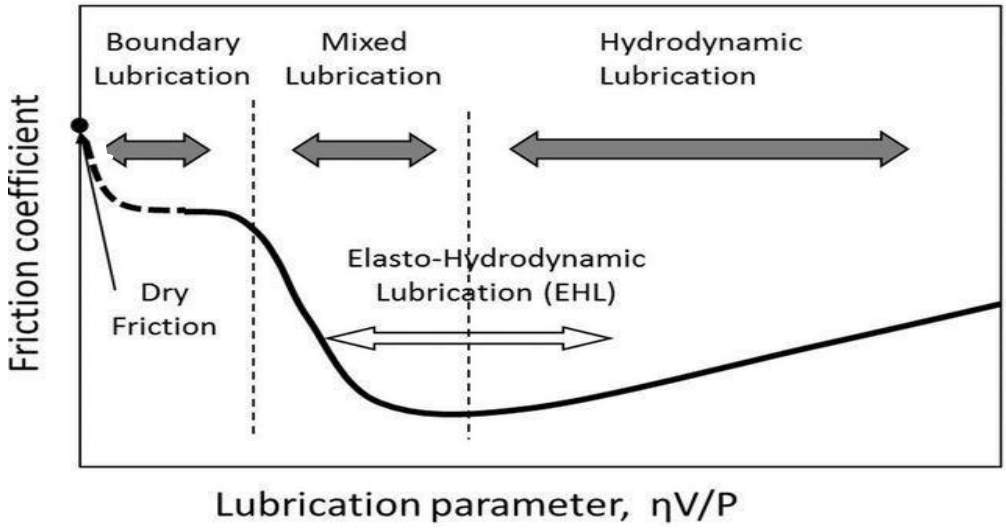

Figure 2: Representation of the Stribeck curve [7].

Figure 2 shows the *Stribeck* curve for a generic lubricant. At the start of the curve, there is no continuity from 0 to some point. This shows that when velocity is zero, this system will not act as a tribo-system [7]. In the *Stribeck* curve, there are three different regions. The boundary lubrication regime, the partial or mixed lubrication regime, and the hydrodynamic lubrication regime.

Boundary Lubrication Regime: The boundary lubrication regime is essentially a solid lubrication. It is associated with metal to metal contact between two sliding surfaces. The lubricant film thickness is negligible. This lubrication is almost like dry lubrication. Reduced lubrication parameter in the boundary lubrication regime leads fluid dynamic lift to almost disappear. As a result, there is a significant amount of contact between sliding surfaces which increases friction in the system. Dry friction is spotted at the end of the boundary lubrication regime [7-9].

Mixed Lubrication Regime: When sliding speed between two surfaces increases, the boundary lubrication is reduced, creating a wedge of lubricant film. The thickness of this film further

increases due to asperities and friction coefficient decreases to the condition known as mix lubrication. This regime of lubrication is called mixed lubrication. There is occasional contact between two sliding surfaces. In this regime, increase in the Hersey number leads to an increase in the thickness of lubricant film between two sliding surfaces [7, 8].

Hydrodynamic Lubrication Regime: The Hydrodynamic lubrication occurs when a full film of oil supports and creates a working clearance between two sliding surfaces. In the hydrodynamic lubrication regime, the lubricant film thickness is comparatively high. There is no contact between two sliding surfaces. The lubricant viscosity plays an important role in maintaining the hydrodynamic lubrication condition. The lower Hersey number corresponds to a low value of viscosity of the lubricant and hence within hydrodynamic lubrication, the friction coefficient is lower when a value of Hersey number is low and friction coefficient is higher when a value of Hersey number is high [7, 8].

Elasto-Hydrodynamic Lubrication: This lubrication regime is kind of hydrodynamic lubrication in which significant elastic deformation of the surface takes place which considerably changes the shape and thickness of lubricant film. In the Electro-Hydrodynamic regime, the friction coefficient is minimum. This regime lies in between mixed lubrication and hydrodynamic lubrication [7].

3.3 Energy Losses Due to Friction and Wear in Different Industries

Friction exists in every type of industry. This friction leads to energy losses and wear of parts and components. The losses caused by friction and wear in industries add to the significant amount of money and energy consumption. Following are the frictional losses associated with some major industries.

3.3.1 Manufacturing and Production industry

The chemical industry and petrochemical industry are the biggest energy consumers worldwide, consuming almost 30% of the total energy used. Another large energy consumer is the iron and steel industry, which accounts for 19% of energy consumption. These two industries consume approximately half of the energy consumed by the industries. Other energy users are cement industry (9%), paper industry (6%), food industry (5%), machinery industry (4%) and non-ferrous metal industry (4%) [10].

In 2013, Holmberg studied the energy losses in the paper machine industry and the mining industry due to friction [11, 12]. The study showed that 25% of total energy consumed is used to overcome the friction in paper mills. On the other hand, in the mining industry energy consumed to overcome friction is about 40% of total energy. The total energy consumed in all manufacturing and production industries to overcome wear losses is estimated to be 14% of the energy used to overcome friction [1].

Figure 3: Production machines in car, food, paper, steel and mining Industry [1].

3.3.2 Transportation Industry

The transportation industry is mainly divided into four categories which are road transportation, sea transportation, rail transportation, and air transportation. Road vehicles use 75% of the total energy used in transportation while the share of rail transportation is 4%. Sea transportation and air transportation consumes 11% each of total transportation energy. For road transportation, 32% of energy is used to overcome friction while it is 10% for the aviation industry and both sea and rail transportation consumes 20% energy to overcome friction. Overall in the transportation industry, 30% of energy is wasted to overcome friction [13, 14]. Table 1 shows the key energy figures for transportation.

Table 1: Key energy figures for transportation industry [1].

Transportation Mode	Global Energy Used EJ/a	Part of global transport energy used %	Energy Used to Overcome Friction %
Road Transport	83	75	32
Rail Transport	4	4	20
Sea Transport	12	11	20
Air Transport	12	11	10
Total	110	100	

3.3.3 Energy Industry

Energy industry includes different types of large power plants, blast furnaces, gas works, and liquefication plants. Energy industry uses a lot of tribological contacts in different components such as turbines, generators, pumps. Holmberg, in 2017, estimated the energy used to overcome friction in the energy industry to be 20% of the total energy used. The losses due to wear are estimated to be 22% of that due to friction [1].

3.4 Technologies to Reduce Friction and Wear

There are different techniques that we use to reduce the friction between two relatively moving surfaces. These techniques are lubricants, new materials, surface modifications, and modern technologies. Following is a summary of these techniques.

3.4.1 Lubricants

Using lubricants is the easiest and cheapest way to reduce friction and wear. Traditionally mineral based oils are used as lubricants but nowadays the use of synthetic based oils is increasing because of their higher thermal stability and longer service life. Tribologist have shown that there are some ways to further improve the properties of traditional lubricants. Some of these techniques are as follows:

A. Nanotechnology-based anti-friction and anti-wear additives:

Addition of specific nanomaterials to traditional lubricants have shown that friction can be reduced in elastohydrodynamic lubricated and boundary lubricated contacts. These contacts can be heavily loaded in certain cases by small pressure also and the oils with nanomaterials still

provide better protection against wear and low shear. Nanodiamonds, carbon nanotubes, graphite onion like carbons are some of the nanomaterials which shows better tribological properties when added to traditional lubricants [15-18].

B. Low Viscosity oils:

In hydrodynamic contacts, viscous and shear losses are significantly high. By using the low viscous lubricant with the same friction resistant and wear resistant properties, these viscous losses can be minimized. Minimizing the viscous losses can save a lot of energy in automotive engines. Polyalkaline glycol-based lubricants are good examples of low viscosity oils with better tribological properties [19–22].

C. Vapor Phase Lubrication:

In vapor phase lubrication a stream of gas takes the lubricant vapor to a mechanical system. In such systems, the volume of lubricant needed for tribological action is very small and is provided by a gas stream. The excessive volume of lubricant causes viscous losses so it is kept away from the mechanical system. Vapor Phase lubrication is useful in high temperature operating systems. Microelectromechanical systems also use phase lubrication [21, 22].

D. Ionic Liquids

Ionic liquids have emerged as very effective lubricants and additives to traditional lubricants in last decade. Ionic liquids contain an organic cation and a relatively weak anion. Ionic liquids show very high temperature stability, low vapor pressure and non-flammability which gives them an advantage over the traditional lubricants. Due to their excellent properties they are not only used

as neat lubricant but also as additives. Ionic liquids used as additives show higher friction reduction compared to traditional additives [25, 26].

E. Other Anti-Wear Additives:

Additives are typically used to protect machine parts from wear and loss of metal during relative motion with other metals. They are polar additives that attach to frictional metal surfaces. When metal to metal contact occurs in mixed or boundary lubrication, they react chemically with metal surfaces. They get activated by heat of contact and form a film that minimizes wear. They also protect the base oil from oxidation and metal from corrosion. These additives are typically phosphorous compounds, with most common being zinc dialkyldithiophosphate (ZDDP) [27].

3.4.2 Materials

Materials have a huge influence on friction as well as wear. Researches to find new more effective materials with better tribological properties have been increased. Along with the search for new materials, there are some techniques which are used to improve material properties. These techniques include case carburizing, nitriding, boronizing in which material hardness, toughness and wear resistance properties are improved. Shot peening and friction stir processing are some of the exotic methods used to enhance material properties. Cold spray process is another new and interesting process to control friction and wear [28].

Apart from above-mentioned surface hardening processes, adding a thin layer of another material on the top surface is also effective in the reduction of friction and wear. This method is

widely used in vacuum chambers with the help of vapor deposition techniques. A thin coating can be further enhanced by nanolayered coatings and using nanostructures [29].

3.4.3 Surface Modifications

Surface roughness and surface topographies of materials have a high influence on tribological properties. Properly designed and controlled surface modifications can reduce friction and wear drastically. This surface modification is called surface texturing and can be very effectively used to minimize the friction [30].

3.5 Surface Texturing

Surface texturing is a surface modification approach resulting in improvement of tribological properties of a material. Texturing makes a positive impact on the loading capacity of materials and friction coefficient. While texturing, artificial microfeatures are created on the surface. Wear debris are trapped in micro dimples and eliminates the plowing friction. Sometimes these dimples can act as a reservoir for lubricant. Because of these properties of micro-dimples, texturing almost reduces the coefficient of friction by 75% for starved lubrication [28–31]. Nowadays the use of textured surfaces is common in a mechanical application like piston rings, thrust bearing, and face seal.

Daniel Braun [35], studied the effect of laser texturing in mixed lubrication regime in which almost 80% friction reduction was seen for optimal dimple diameter of textured surface. This study also showed that there is nonlinear dependence of friction coefficient on dimple diameters, sliding speed and oil temperature.

Texturing the surface also shows positive variation in the *Stribeck* curve. The textured surfaces produced by modulation assisted machining accelerates the appearance of the elasto-hydrodynamic regime with friction reduction of 56% and wear reduction of 90%. In the figure 4 below, you can see the hydrodynamic lubrication region is enlarged which is a good sign [36].

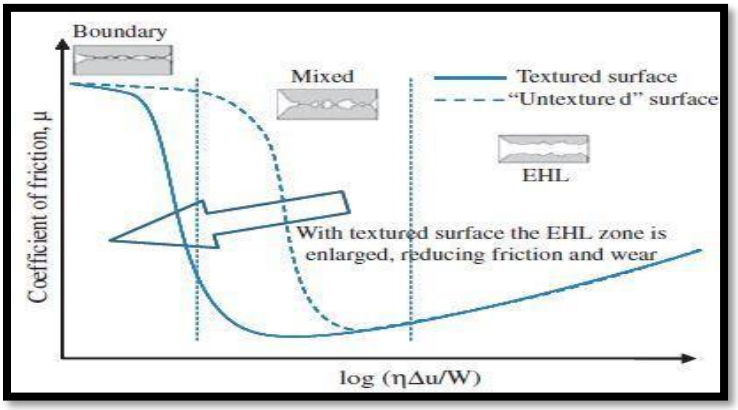

Figure 4: variation in stribeck curve due to surface texturing [37].

Depending on the design parameters, the effectiveness of surface texturing varies. Design parameters can be size, shape, density or features such as speed and load [38].

Haiwu Yu [39], studied the geometric shape effects of textured surfaces on generation of hydrodynamic pressure between two contacting surfaces. Test were performed on circular, triangular and elliptical textured surfaces which showed that the textured surface with elliptical dimples shows the highest load carrying capacity over other shapes.

Figure 5 shows different shapes of textured surfaces. Each shape provides different tribological properties and response [39].

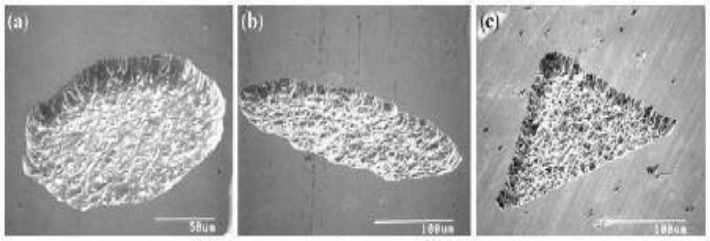

Figure 5: Different types of textured surfaces (a) circle, (b) Ellipse, (c) Triangle [39].

Numerous techniques have been identified to modify surfaces and reduce the friction. Textured surfaces are successful or not is decided by following two main factors.

A. Achieving maximum efficiency by optimizing design pattern.
B. A cheaper surface texturing technique which can be implemented in mass production.

In the last two decades, lots of efforts have been taken to optimize design patterns which will give high load-bearing capacity with minimum friction. These parameters are nothing but shapes, sizes or speed and load [40].

3.6 Manufacturing Techniques for Textured Surfaces

Over the years, a wide range of textured surface manufacturing techniques has evolved. The purpose of these wide range techniques is to develop an optimum surface texturing pattern which will reduce the friction [37].

Selection of manufacturing technique depends on its simplicity, manufacturing speed, cost and flexibility to produce. Following are manufacturing processes for textured surfaces [40]:

A. Material Addition: In this process, the material is added to create patterns on the surface which result in areas of reliefs.

B. Material Removal: In this process, the material is removed to create patterns on surfaces which result in depressions.

C. Moving Material: In this process redistribution of material from one part to another part takes place.

D. Self-Forming by wear: As a result of wear resistance, a textured is formed on the surface.

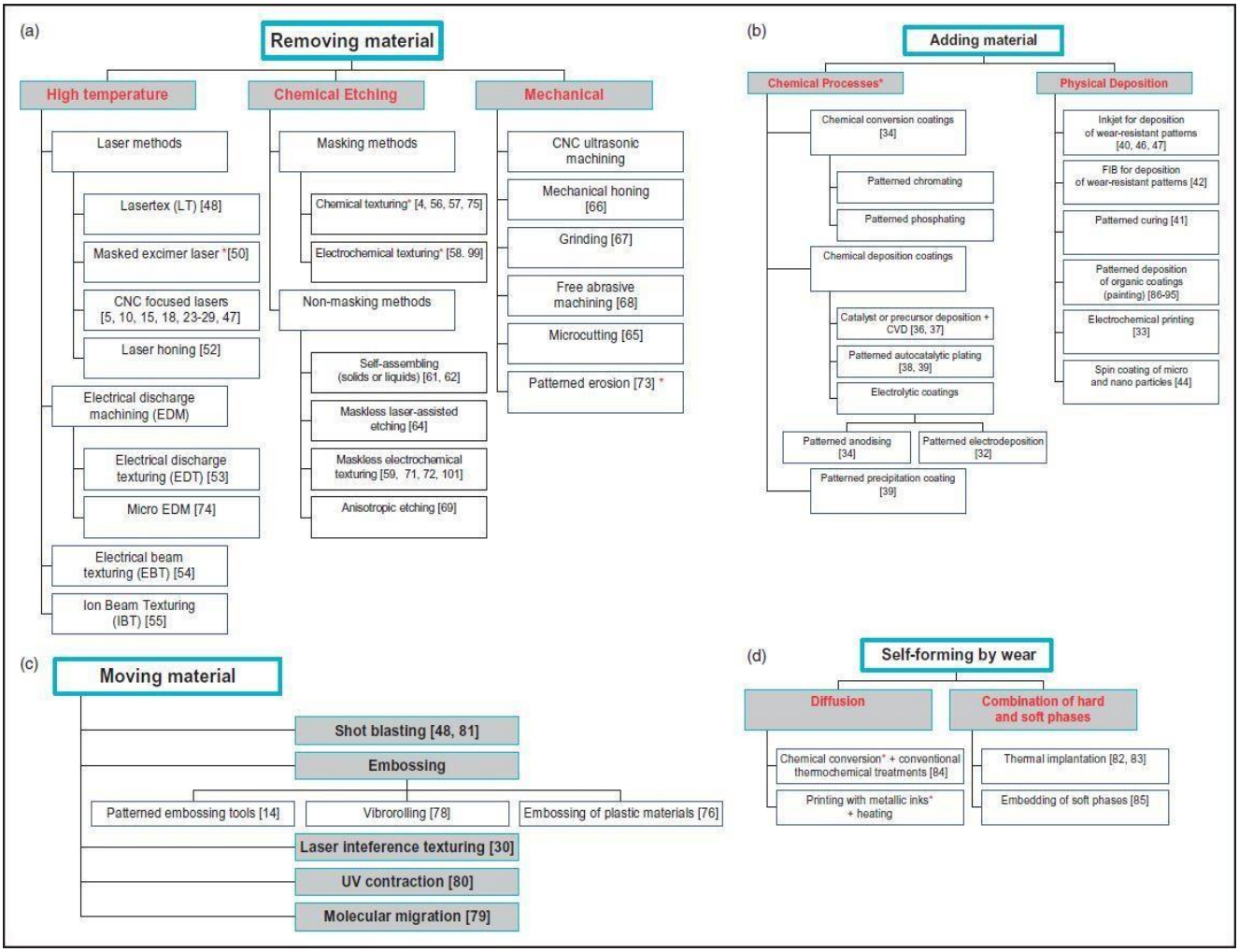

Figure 6: Schematic representation of the tree structure of surface texturing techniques in use currently [40].

Figure 6 shows the list of current manufacturing techniques of textured surfaces.

The oldest technique used for texturing is sandblasting. It includes bombarding of very small solid

particles at high speed across the surface of the material. It is very cost effective and easy to implement but controlling the depth and density of texture pattern is difficult. This limits the use of sandblasting technique to very few applications [32, 33].

Photolithography and ion beam are other techniques which produce textured surfaces with high precision in nano-scales. This technique needs a vacuum for its operation which limits its use to highly specialized workplace. The production cost is high and it's not suitable for mass production. Another disadvantage with this technique is that it cannot texture non-flat surfaces [42].

The use of a mechanical system of surface texturing which uses a two-ball end mill to texture the surfaces was studied by Matsumura et al [43]. This is a highly efficient texturing technique with machining error of only ±7 microns. If the revolutions of workpiece and tool feed rate are high, then dimples can be machined independently.

Schneider [44] tested another technique called vibrorolling technique. This technique is getting popular since the 90's. Increased contact rigidity and fatigue strength are the advantages of this technique. It gives quick and optimized surface finish because of its independence of service characteristics like dimension, shape, positioning and surface area. Also, this machine does not need a complex setup of machining elements as it uses current conventional machining platforms.

The vibromechanical texturing technique uses CNC lathe with piezo-electric actuated tools which generate dimple indentions. Though this process showed an 11%-dimensional error for aluminum, it was 90% for steel. This error could be eliminated by the closed-loop control system [45].

The most common methods used today is the Laser Surface Texturing Technique. Etsion et al, Braun et al, Scaraggi et al [3], did the extensive research to study this technique. It produces patterns with small features, with a depth of approximately 200 nm and diameter of 20 microns can be easily machined. It is comparatively fast and non-hazardous to an environment having uses in multiple types of contacts. Laser texturing is a digital process which gives you consistency with surface finishing. A fully digital process that also permits you to the creation of new texture patterns which are difficult to do with other texturing methods. Another plus point of laser texturing is that it offers flexibility in dimple depths and diameters. The disadvantage with this method is burr formation around the dimple circumference and hence need of post processing [46].

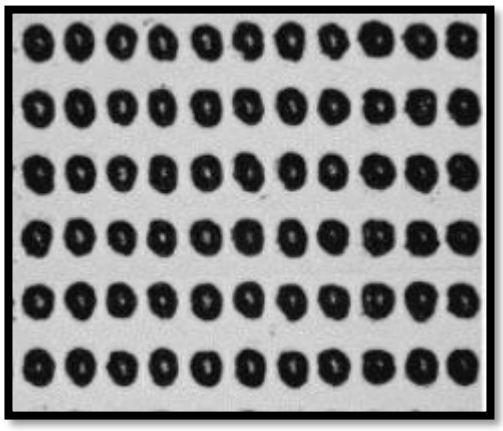

Figure 7: Typical laser textured surface [47].

Figure 7 shows the typical laser textured surface. In this thesis, samples manufactured by laser texturing technique will be used to perform tribological tests. These samples were prepared by professor Jorge Salguero from Cadiz university in Spain.

4.0 OBJECTIVES OF THE PROPOSED WORK

The objectives of this research work are:

1. To study the effect of laser texturing on tribological properties of titanium-ceramic contact.
2. To study the influence of the laser speed on the dimple density.
3. To study the effect of variation of dimple density on the tribological properties of titanium alloy Ti6Al4V.
4. To find the dimple density which will give maximum reduction in friction and wear.

5.0 EXPERIMENTAL DETAILS

5.1 Samples

In this study, Ti6Al4V titanium alloy is used as a sample material. Ti6Al4V is a titanium alloy which is widely used in direct manufacturing of parts and prototypes for racing and aerospace industry. Its high strength low weight ratio and outstanding corrosion resistance make it suitable for many biomedical applications too. Table 2 shows the different elements present in a Ti6Al4V alloy with their percentage.

Table 2 : Percentage of different elements in Ti6Al4V alloy.

Element Name	Percentage of it in Ti6Al4V
Titanium	90%
Aluminum	6%
vanadium	4%
Iron	0.25%
Oxygen	0.2%

The laser texturing process is used to texture the surface. A Rofin EasyMark F20 machine is used to texture the surface. Using eight different laser velocities, eight different samples with varying dimple densities are manufactured on a single plate of Ti6Al4V metal. The dimensions of the plate

are 50 mm in length, 48 mm in width, and 5 mm in height. Every single sample has a length of 10 mm and a width of 10 mm as shown in Figure 8.

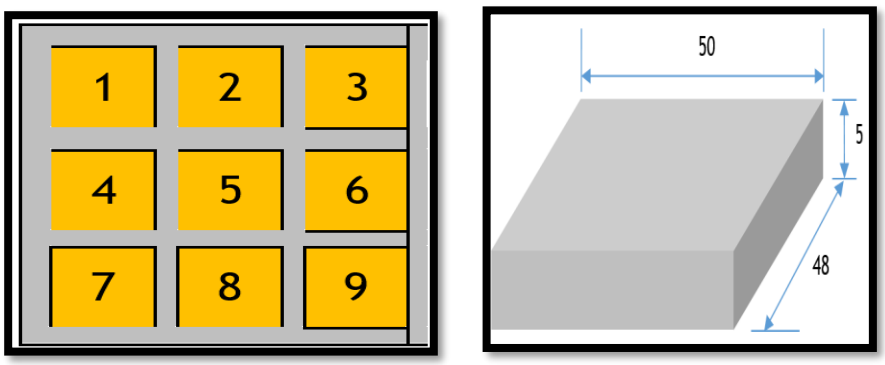

Figure 8: Schematic representation of the sample (dimensions are in mm).

As the laser processing velocity changes, the dimple density also changes. The dimple density is calculated using laser speed and laser frequency. The lower the laser processing velocity, the higher the dimple density is. There are eight different textured surfaces with different dimple densities on the metal plate that used for the frictional tests.

Sample 1 was created with lowest laser speed of 400mm/s and highest dimple density of 50dimples/mm. Sample 2 through sample 8 were created by using the laser speed ranging from 800mm/s to 2800mm/s respectively, giving out the dimple densities ranging from 25dimples/mm to 7.1dimples/mm. Sample 9 is untextured sample of Ti6Al4V. Different manufacturing parameters for given samples are shown in Table 3.

Table 3: Parameters used for texturing the samples.

Sample No.	Laser Spot Size (microns)	Laser Speed (mm/s)	Dimple Density (dimples/mm)	Laser Frequency (Hz)	Spacing between two laser passes (microns)
Sample 1	60	400	50	20000	20
Sample 2	60	800	25	20000	40
Sample 3	60	1200	16.7	20000	60
Sample 4	60	1600	12.5	20000	80
Sample 5	60	2000	10	20000	100
Sample 6	60	2400	8.3	20000	120
Sample 7	60	2600	7.6	20000	140
Sample 8	60	2800	7.1	20000	160
Sample 9	Untextured	-	-	-	-

Figure 9 (a) shows the schematic representation of variation of dimple density and Figure 9 (b) shows the actual metal sample which is used for the tests. Sample 1 has the highest dimple density while sample 8 has the lowest.

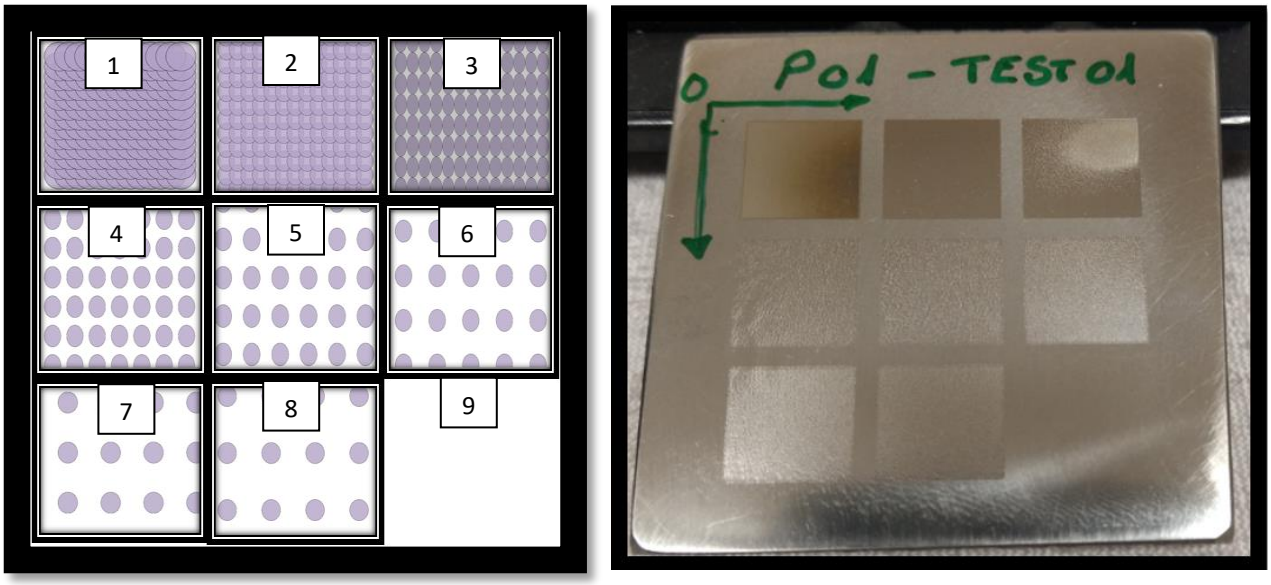

(a) *(b)*

Figure 9: (a) Schematic representation of variation in dimple density (b) Variation of dimple density on the actual sample.

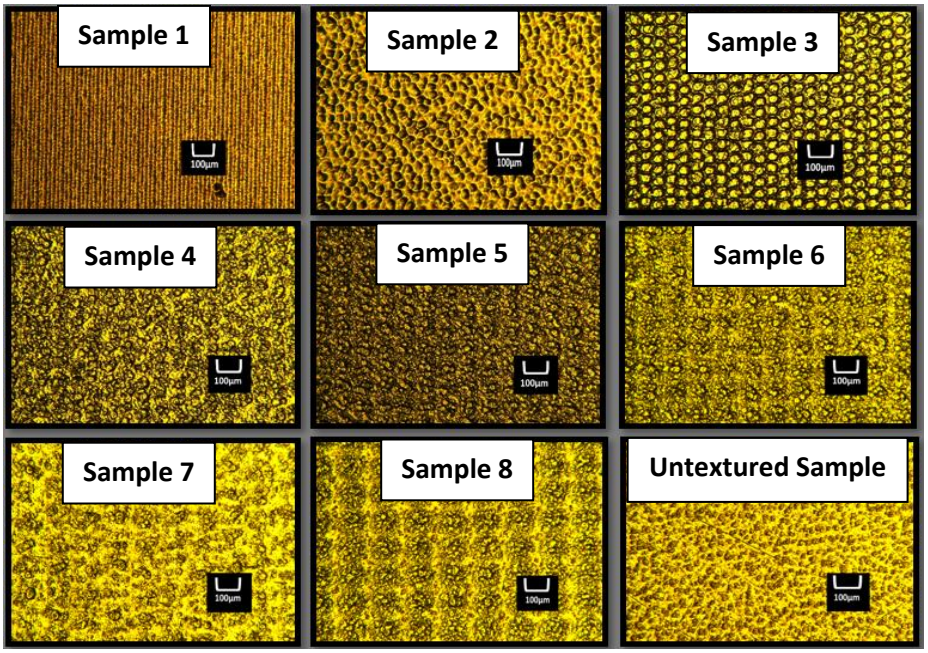

Figure 10 : Microscopic images of the samples.

Figure 10 shows the microscopic images of the samples used to perform the tests. Sample 1 with the highest dimple density, sample 8 with the lowest dimple density and sample 9 which is the untextured surface of the titanium.

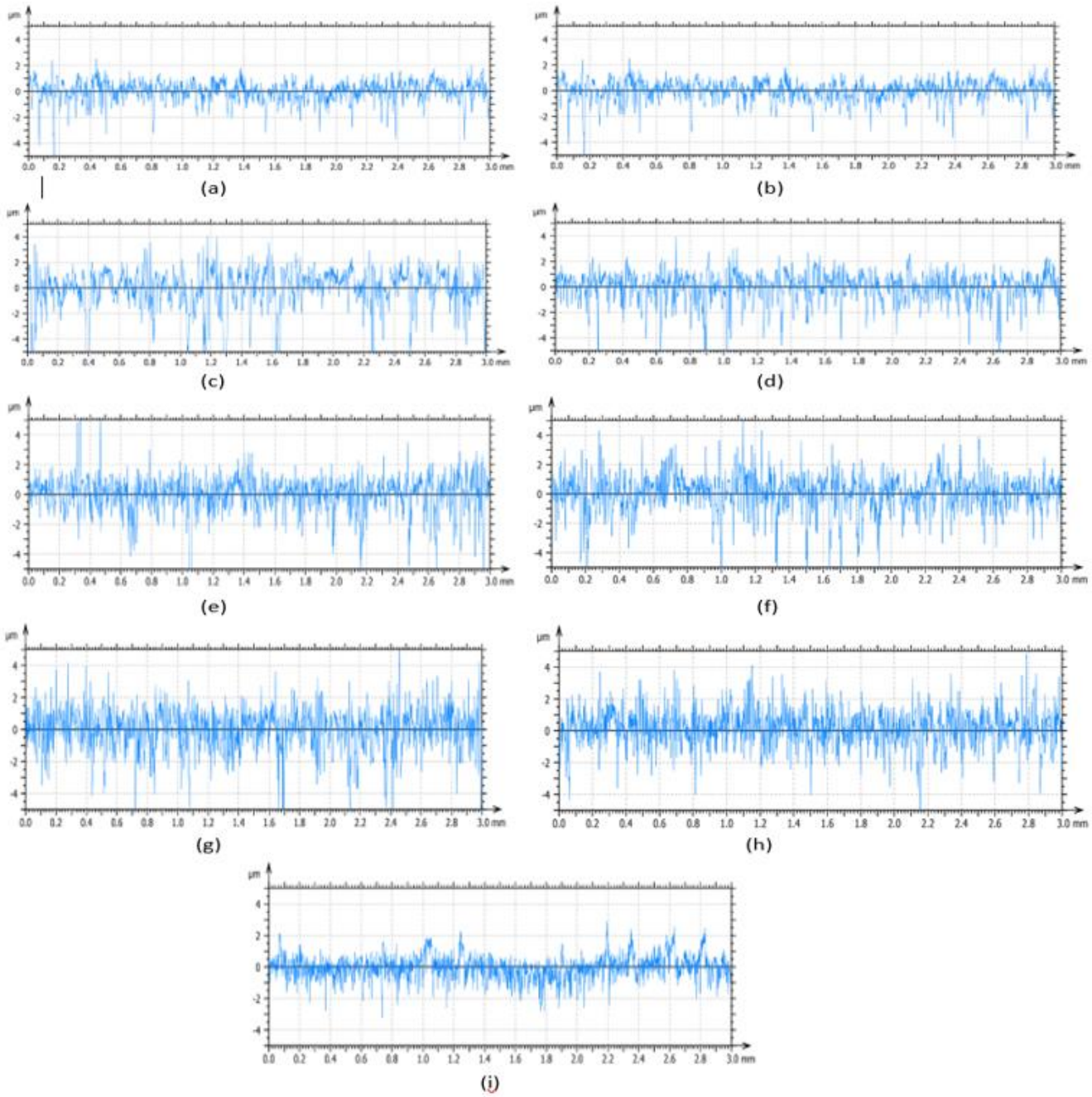

Figure 11 : Surface profiles of all the samples (a)Sample 1 (b)Sample 2 (c)Sample 3 (d)Sample 4 (e)Sample 5 (f)Sample 6 (g)Sample 7 (h)Sample 8 (i)Untextured

Figure 11 shows the 2D surface profiles of the untextured and textured samples. Sample 1 with lowest laser speed sample 8 with highest laser speed and sample 9 is untextured sample. The 3D images of surface characterization for all the samples can be seen in Appendix-II.

Table 4: Dimple Depths for all the samples

Laser Speed	Dimple Depth (microns)
400mm/s (Sample 1)	6
800mm/s (Sample 2)	6
1200mm/s (Sample 3)	8
1600mm/s (Sample 4)	7
2000mm/s (Sample 5)	7
2400mm/s (Sample 6)	7
2600mm/s (Sample 7)	8
2800mm/s (Sample 8)	7
Untextured Sample	_

Table 4 shows the dimple depths for all the samples measured by the NANOVEA non-contact profilometer. The dimple depths for all the samples range from 6µm to 8µm, which is more or less similar for all the samples.

5.2 Contact Angle

Wettability is the property of fluid to spread on or adhere to a solid surface. This wettability is generally measured in terms of the contact angle which fluid makes with the surface. If contact angle of fluid is lower, then the wettability of fluid is higher. Higher wettability of lubricant with the metal surface gives better friction reduction [48]. Figure 12 shows the measurement of contact angle.

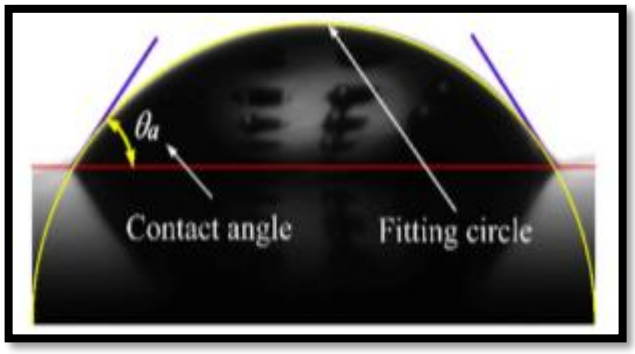

Figure 12: Contact angle of lubricant drop with surface[48]

The surface texturing affects the wettability of metal surfaces. To study the effect in wettability the contact angle tests were performed on each sample using RAME-HART's Goniometer and Drop-Image software. PAO is used as a liquid over the Ti6Al4V textured surface. These tests were conducted using 2 microliters of PAO for around 24 seconds to collect 25 data points of contact angles for each sample on Ti6Al4V.

5.3 The Roughness of Textured Surfaces

Roughness tests were performed on all the samples for Ra, Rz, Rpk values using the NANOVEA ST400 non-contact profilometer with lateral resolution of 1.7 micro-meter and vertical resolution of 8 nano-meter. Ra being the arithmetic average of the absolute values of the roughness profile ordinates, Rz is the arithmetic mean value of the single roughness depths of consecutive sampling lengths and Rpk is Maximum Profile Peak Height. These roughness values were studied against the laser processing velocity.

5.4 Surface Hardness Tests

Though laser texturing has several advantages over different texturing processes, it generates heat while texturing process is underway. As a result of a generated heat, the surface of the metal sample may be heat treated which can increase the surface hardness of it. This increase in surface hardness due to unwanted heat treatment impacts the tribological properties of the material. In our study, we want to focus only on surface texturing and not on surface hardening. Therefore, to investigate the surface hardening due to laser texturing, surface hardness tests were performed on Vicker's micro hardness tester. For each sample, twenty five readings were recorded at different locations inside the sample.

5.5 Tribometer Tests

Tribometer tests were performed to calculate the friction coefficient and wear on the titanium surface. The reciprocating ball-on-flat tribometer with Tungsten-Carbide ball was used to conduct the tests with PAO as a lubricant. Each test was performed under the same operating conditions with the normal load 5 N which corresponds to maximum contact pressure of 3.8 GPa. The frequency used is 2 Hz with a stroke length of 3mm, and a total sliding distance of 50 m. Figure 13 shows the tribometer used to perform the tests.

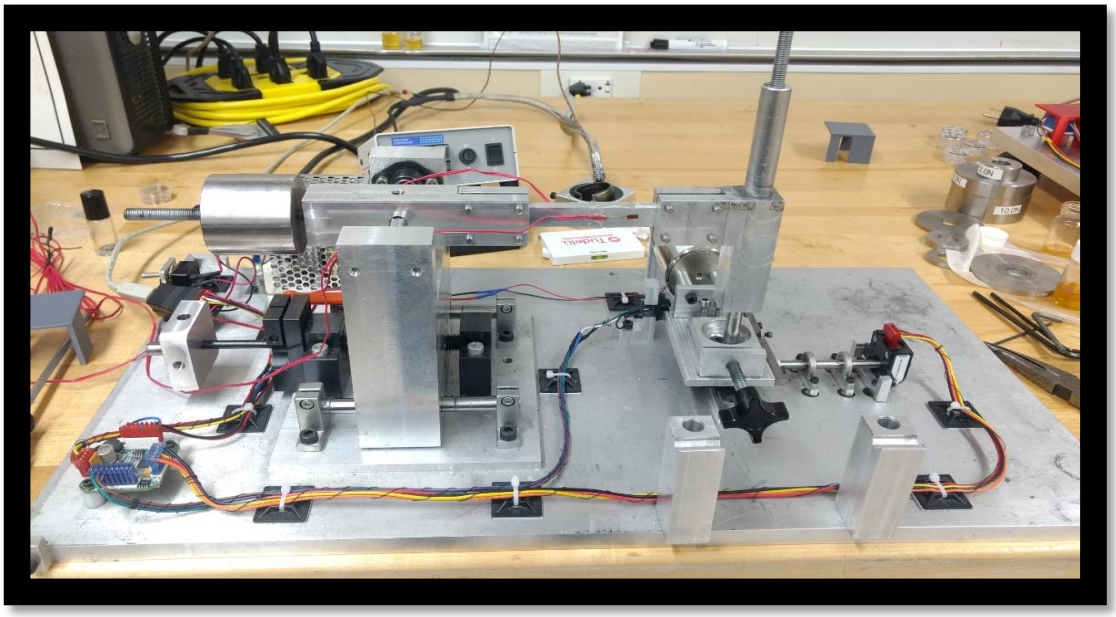

Figure 13: Tribometer used to conduct the tests.

In ball on flat reciprocating tribometer, a tungsten carbide ball is inserted inside the pin holder which rests on the titanium sample surface. Then reciprocating movement is provided to the pin which causes friction between tungsten carbide ball and titanium surface. Due to this friction,

there is instantaneous deflection in the tribometer arm which is recorded using strain gauges. This strain gauge reading is then converted into friction coefficient using a LabVIEW program.

After performing the tribometer tests, wear tracks were analyzed using OLYMPUS B-2 optical microscope. Using the same microscope wear track widths were also measured. Then wear volume for these tests was calculated using the equation 2 [49]:

$$V_f = L_s \left[R_f^2 \arcsin\left(\frac{W}{2Rf}\right) - \frac{W}{2}(R_f - h_f)\right] + \frac{\pi}{3} h_f^2 (3R_f - h_f) \qquad \text{Equation (2)}$$

Where V_f is a wear volume in mm^3, L_s is stroke length in mm, W is wearing track width in mm, R_f is the radius of the ball in mm and h_f is wear depth in mm which is calculated from the equation 3 [49].

$$h_f = R_f - \sqrt{R_f^2 - \frac{W^2}{4}} \qquad \text{Equation (3)}$$

For each sample at least 2 tests were performed to guarantee the repeatability of the results.

6.0 RESULTS

6.1 Wettability

The graph in Figure 14 shows that the contact angle test results for all the samples. It is clear that the contact angle for the untreated sample is higher compare to textured surfaces. The decrease in contact angle for textured surfaces shows higher wettability of liquid towards textured surfaces which is favorable for friction reduction. Sample with laser velocity 800mm/s (sample 2) and 2400mm/s (sample 6), shows the lower contact angle values.

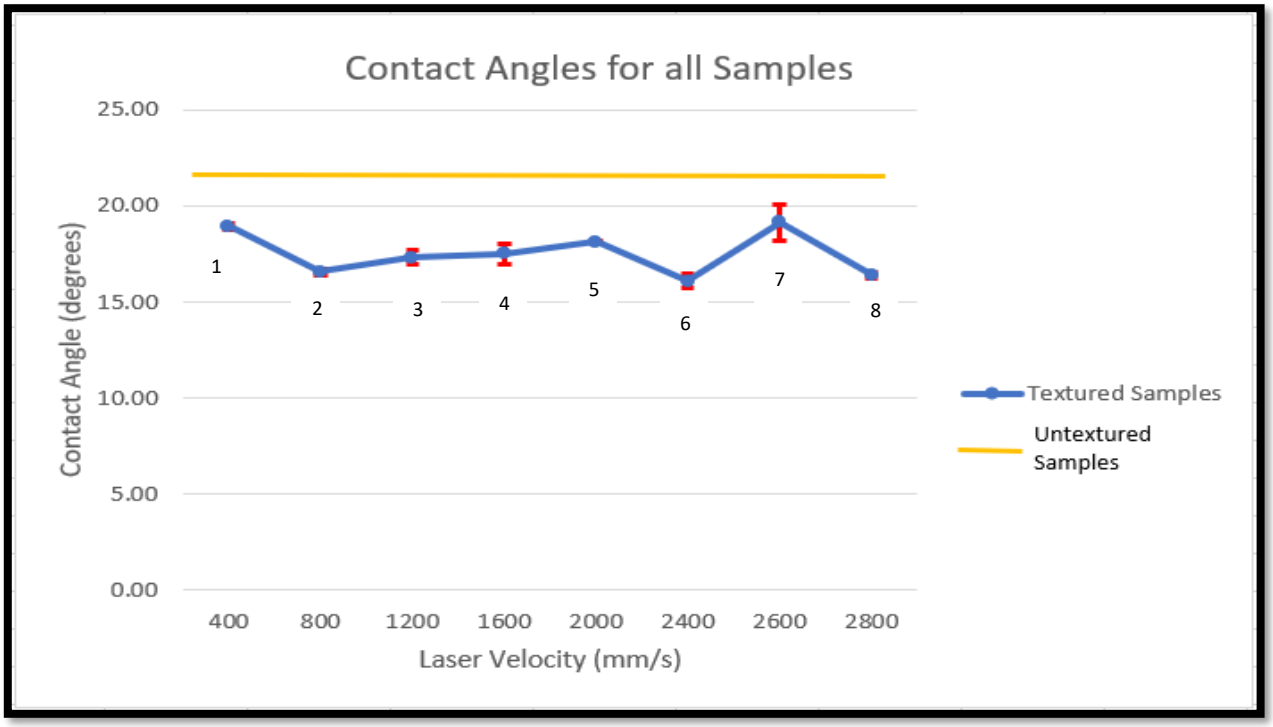

Figure 14 : Contact angles for all the samples.

6.2 Surface Roughness

Figure 15, 16 and 17 shows the roughness test results for all the samples. The yellow line in the figure represents the value for untextured surface

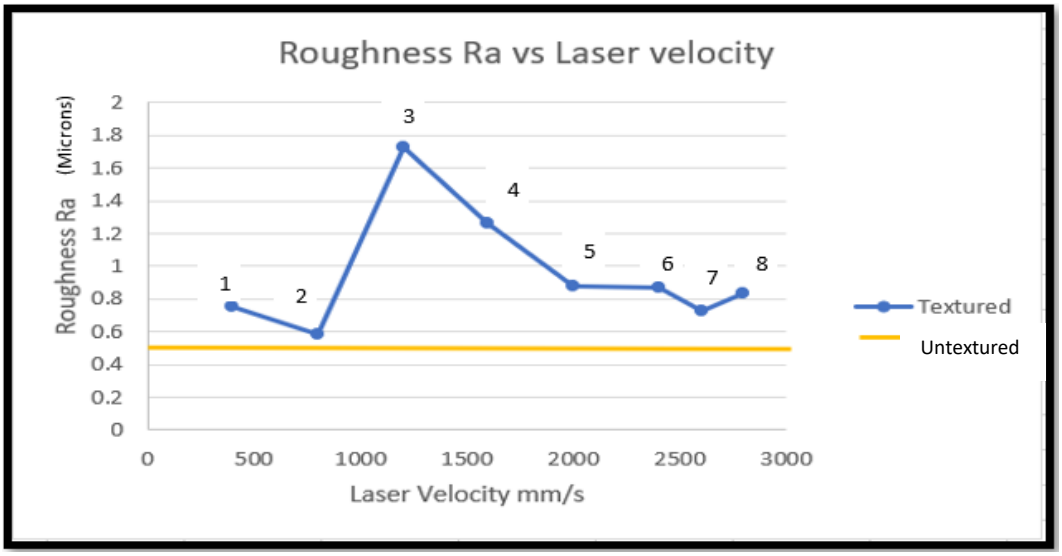

Figure 15 : Roughness value Ra for all the samples.

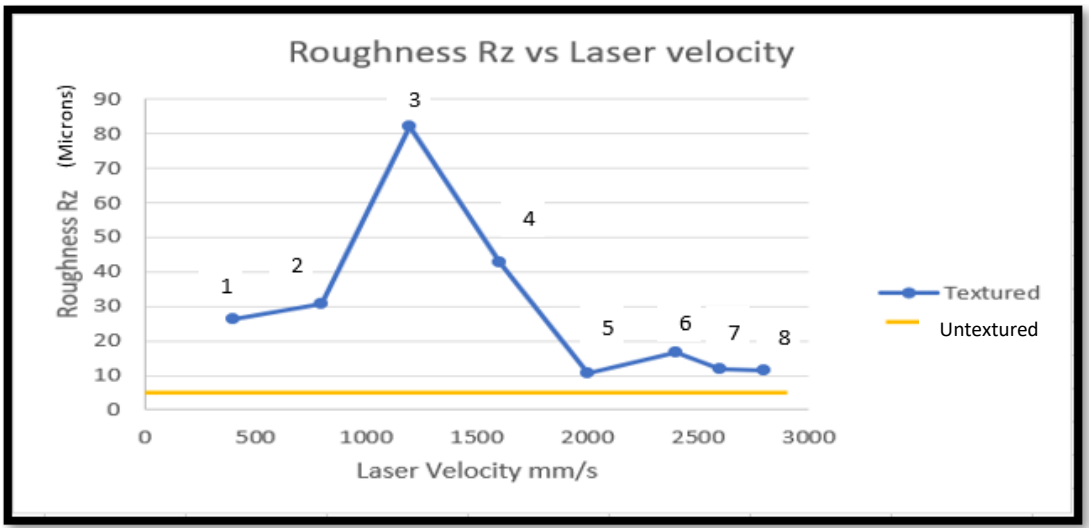

Figure 16 : Roughness value Rz for all the samples.

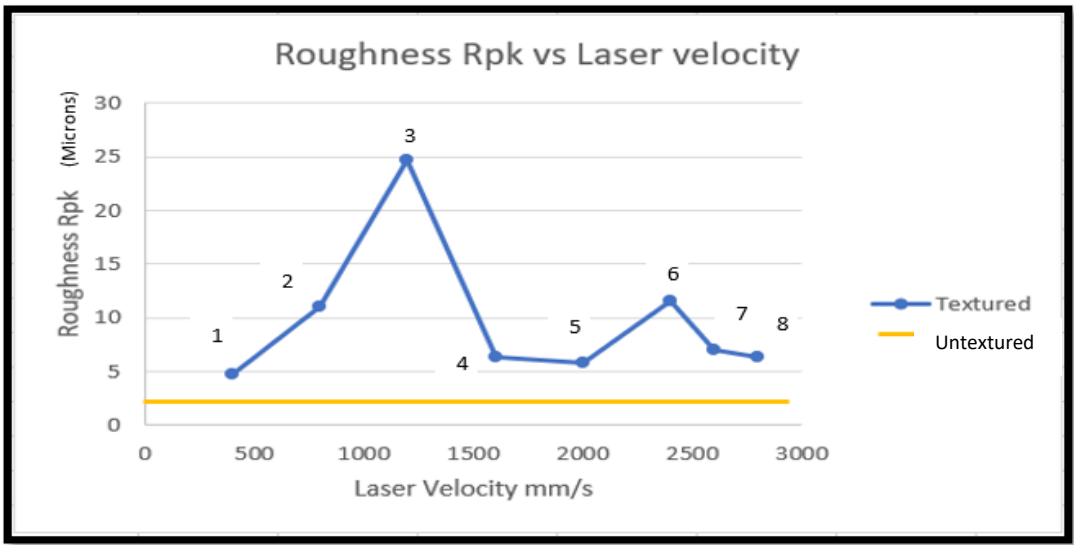

Figure 17 : Roughness value Rpk for all the samples.

It is clear that the roughness of the untreated surface is lower than textured surfaces as expected. Sample with laser speed 1200mm/s (sample 3), shows high values of roughness for all the three roughness behaviors which are Ra, Rz, Rpk. This is because, dimples are located very tightly to each other and there is no empty space between two consecutive dimples

6.3 Surface Hardness

Figure 18 shows the surface hardness test results for all textured surfaces. From figure 14, sample with lower laser speed of 400mm/s (sample 1), shows higher surface hardness because it is exposed to the laser for a longer time as compared to other samples. Samples with laser velocity ranging from 1200mm/s to 2800mm/s (sample 3 to sample 8), shows similar surface hardness as untextured surface and sample with laser velocity 800mm/s (sample 2), shows slightly increased surface hardness.

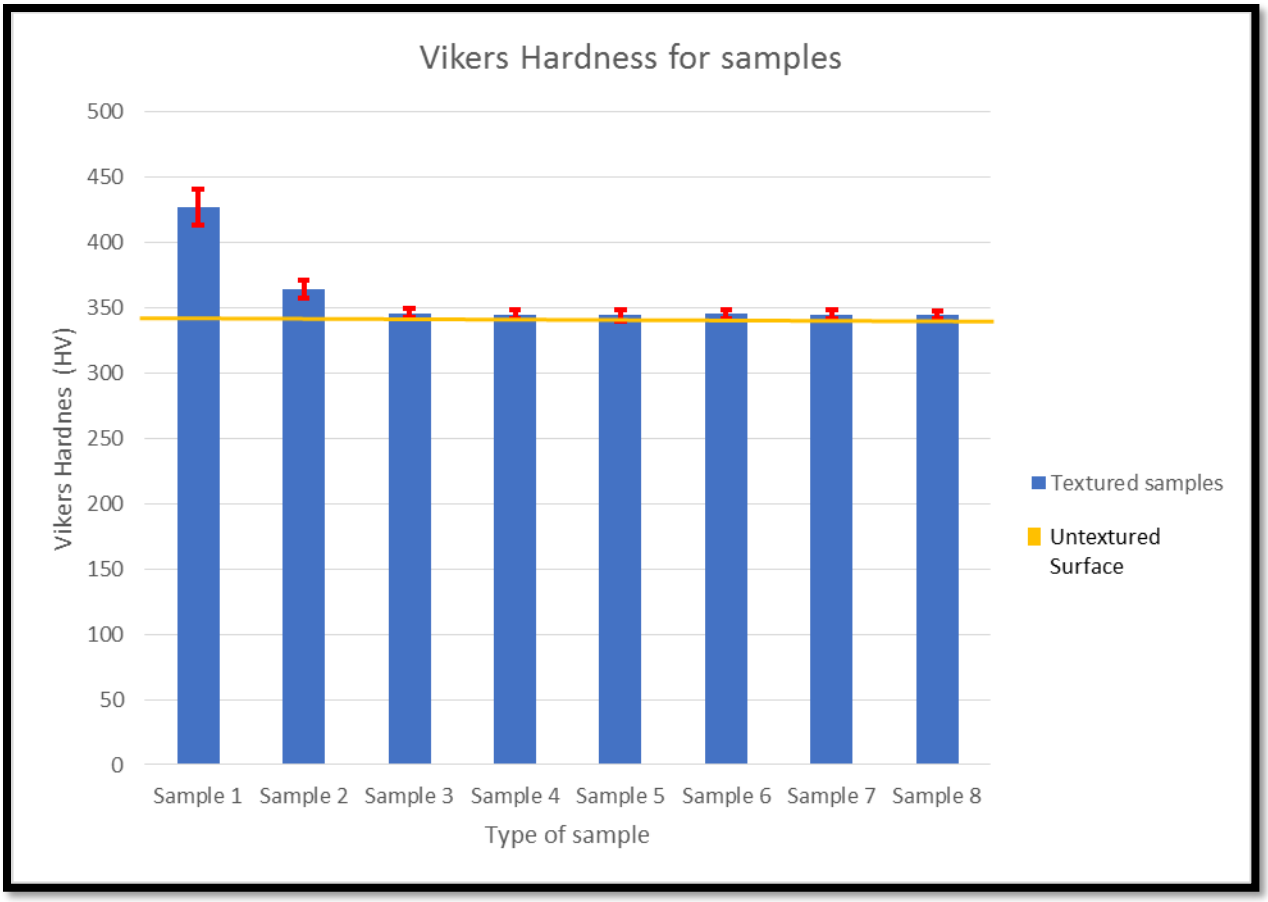

Figure 18 : Hardness test results for all the samples.

6.4 Tribological results

Figure 19 shows the friction coefficient values obtained from tribometer tests. The yellow line represents the friction coefficient for untextured sample. Friction coefficient for textured surfaces is reduced compared to untextured sample. Samples with laser velocity 400mm/s and 800mm/s (sample 1 and sample 2) and highest dimple density show the lowest friction coefficient (0.1241 and 0.1269 respectively) whereas the untextured sample has the highest friction coefficient (0.3808). Samples with laser velocity ranging from 1200mm/s to 2800mm/s (Sample

3 to sample 8), have almost similar friction coefficient which is lower than the untextured sample with average reduction in friction of 6%.

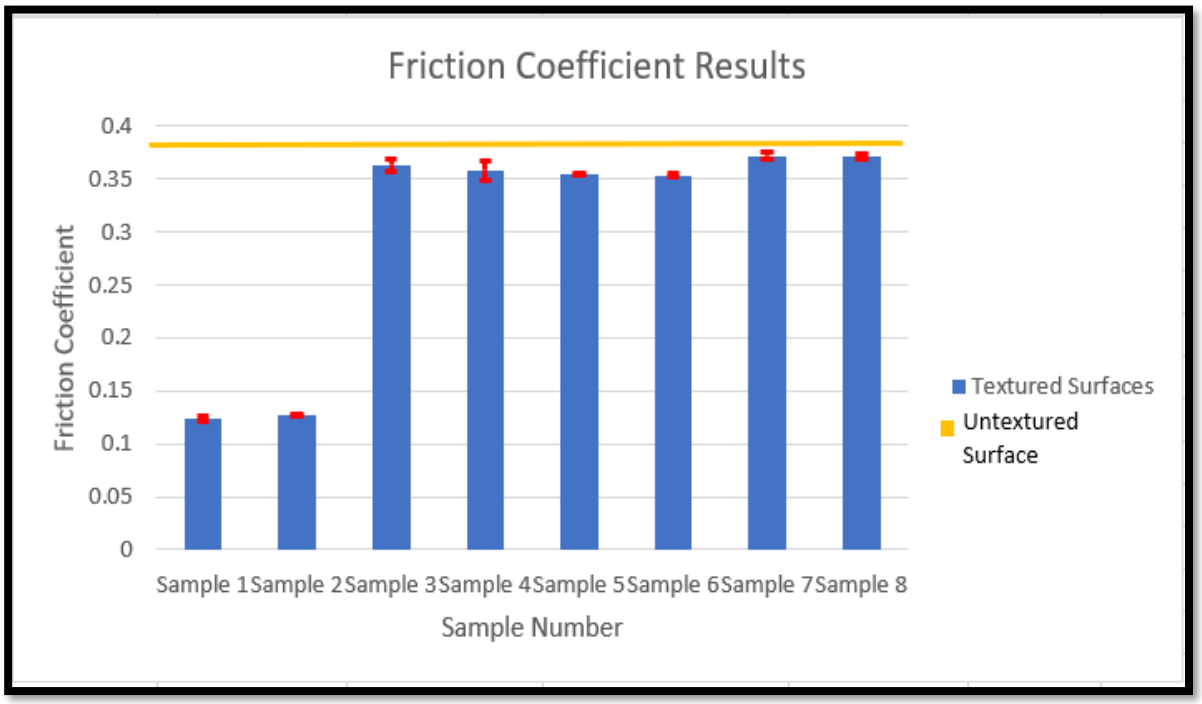

Figure 19 : Friction coefficient of different samples

As compared to the untextured surfaces, samples with laser speed of 400mm/s and 800mm/s (sample 1 and sample 2) shows friction reduction of around 67%. However, for the sample with laser speed of 400mm/s and dimple density of 50dimples/mm (sample 1), the surface hardness is increased considerably due to longer exposure to laser which can affect the tribological properties and the friction reduction is not because of only surface texturing. While the second sample with laser speed of 800mm/s and dimple density of 25dimples/mm (sample 2), shows very low increase in surface hardness. It can be said that the reduction in friction is due to laser texturing.

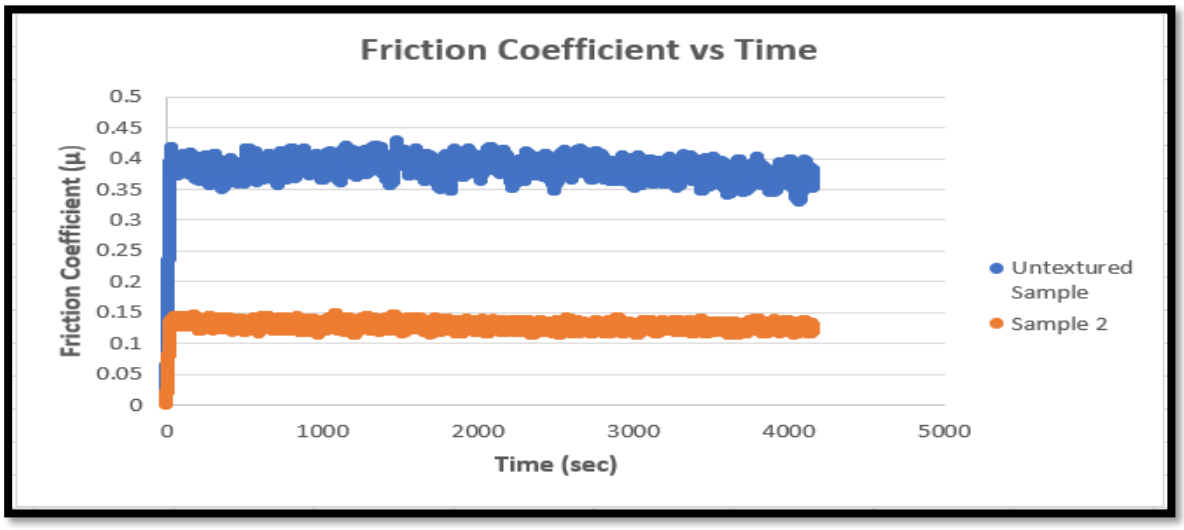

Figure 20: Friction vs Time curve for sample with laser speed 800mm/s and dimple density of 25dimples/mm (sample 2) and untextured sample

Figure 20 shows the reduction in friction for the sample with laser speed of 800mm/s and dimple density of 25dimples/mm (sample 2), as compared to untextured sample.

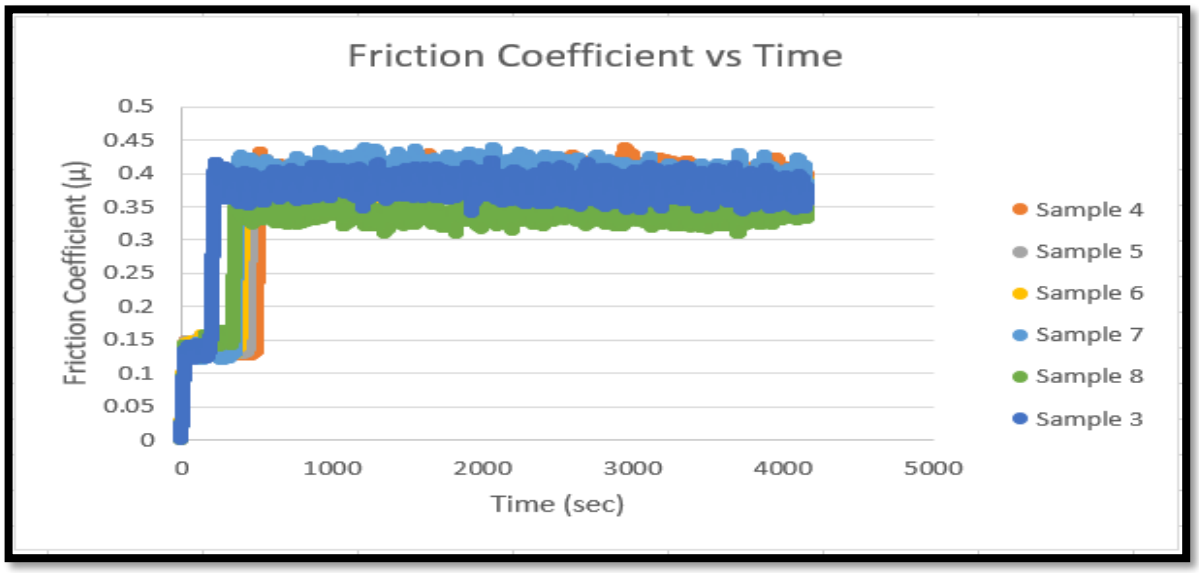

Figure 21: Friction coefficient vs time curve for samples with laser speed ranging from 1200mm/s to 2800mm/sec (sample 3 to sample 8).

Figure 21 shows the friction coefficient vs time curves for samples with laser speed ranging from 1200mm/s to 2800mm/s (sample 3 to sample 8). From the figure, a step in a friction coefficient graph can be seen. The reason behind this step is wearing out of dimples. While the test is in process, at first, there are dimples on the surface and friction coefficient stays low for that time period due to texturing but after some time these dimples wear out and the metal surface starts acting as an untextured surface with an increase in the friction coefficient. Friction coefficient curves for each sample can be seen in Appendix-1.

The dimple wearing out time for all the samples was noted. Table 5 shows the dimple wearing out time for given samples.

Table 5: Dimple wearing out time for given samples.

Laser Speed (mm/s)	Time to Wear Out Dimples (sec)
1200 (Sample 3)	150
1600 (Sample 4)	506
2000 (Sample 5)	442
2400 (Sample 6)	390
2600 (Sample 7)	355
2800 (Sample 8)	337

It can be seen from table 5 and figure 22 that dimple wearing out time for sample with laser speed 1200mm/s (sample 3) is lowest due to the highest surface roughness of this sample amongst all the samples. For samples with laser speed ranging from 1600mm/s to 2800mm/s

(sample 4 to sample 8), this time is decreasing with higher time for sample with laser speed of 1600mm/s (sample 4) and lowest time for sample with laser speed of 2800mm/s (sample 8). For these samples dimple density decreases from 12.5dimples/mm to 7.1dimples/mm which results in decrease in dimple wearing out time.

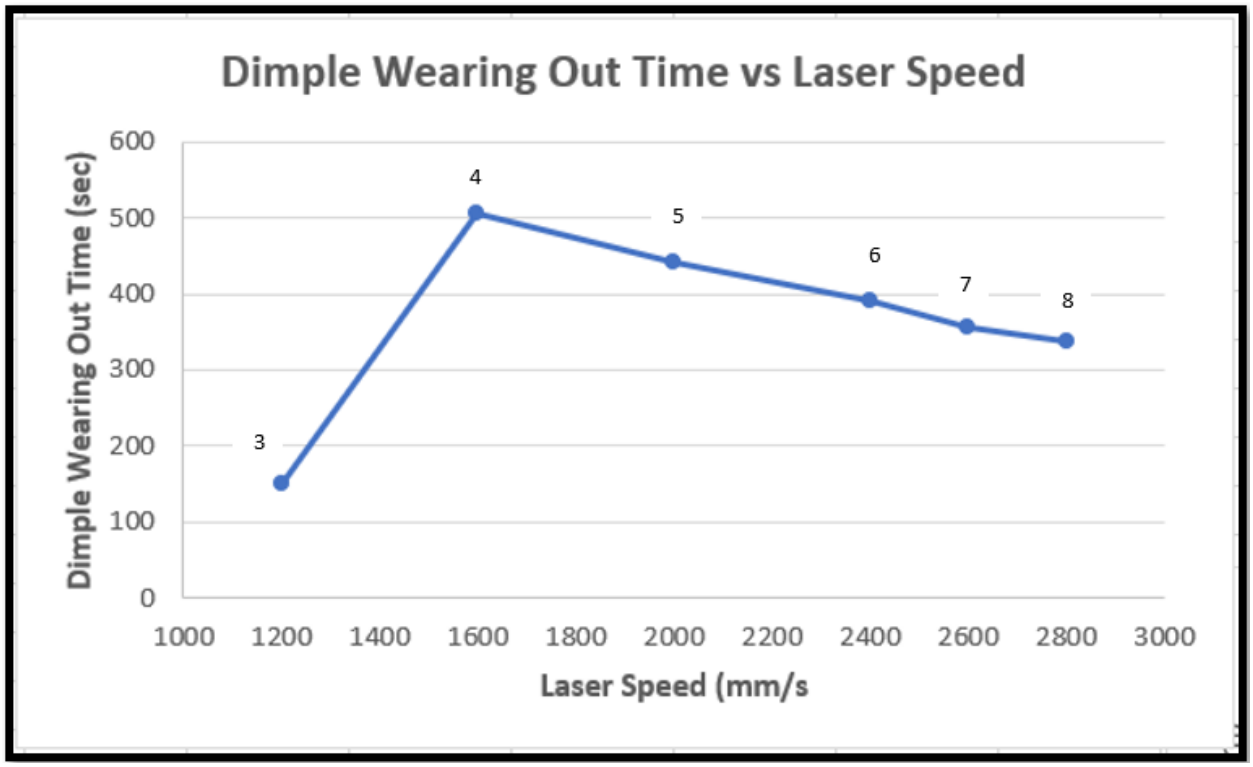

Figure 22 :Dimple wearing out time for given samples.

Figure 22 shows the graph of dimple wearing out time vs laser speed used for texturing the samples.

Figure 23 shows the wear volume results for all the samples. Yellow line indicates the friction coefficient for untextured sample. It is clear that the wear volume for textured surfaces is reduced. Wear volume for samples with laser speed of 400mm/s and 800mm/s (sample 1 and sample 2) is reduced by almost 99% as compared to untextured sample. However, the sample with laser speed of 400mm/s and dimple density of 50dimples/mm (sample 1), is exposed to laser for longer time which results in the increase of surface hardness. This increased surface hardness can be one of the reasons to reduce the wear for this particular sample. While the second sample with laser speed of 800mm/s and dimple density of 25dimples/mm (sample 2), shows very low increase in surface hardness and it can be said that the reduction in wear is due to laser texturing. Samples with laser velocity ranging from 1200mm/s to 2800mm/s (Sample 3 to sample 8), have almost similar wear volume which is slightly lower than the untextured sample with average reduction in wear volume of 11%.

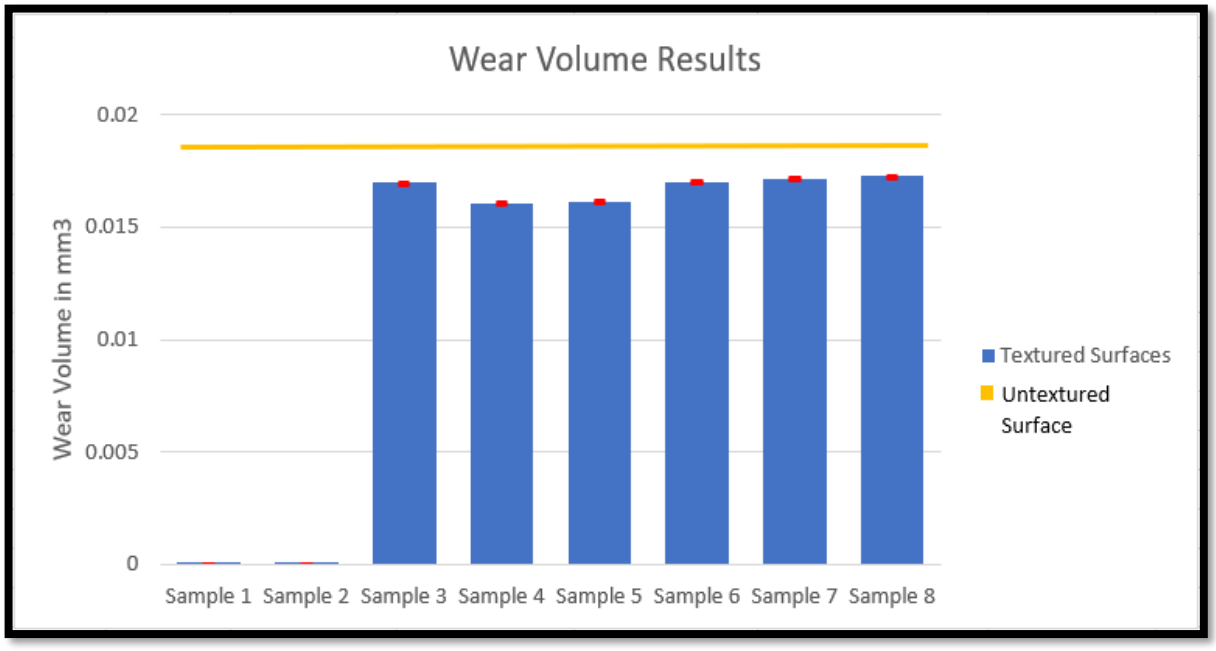

Figure 23: Wear volume for all the samples.

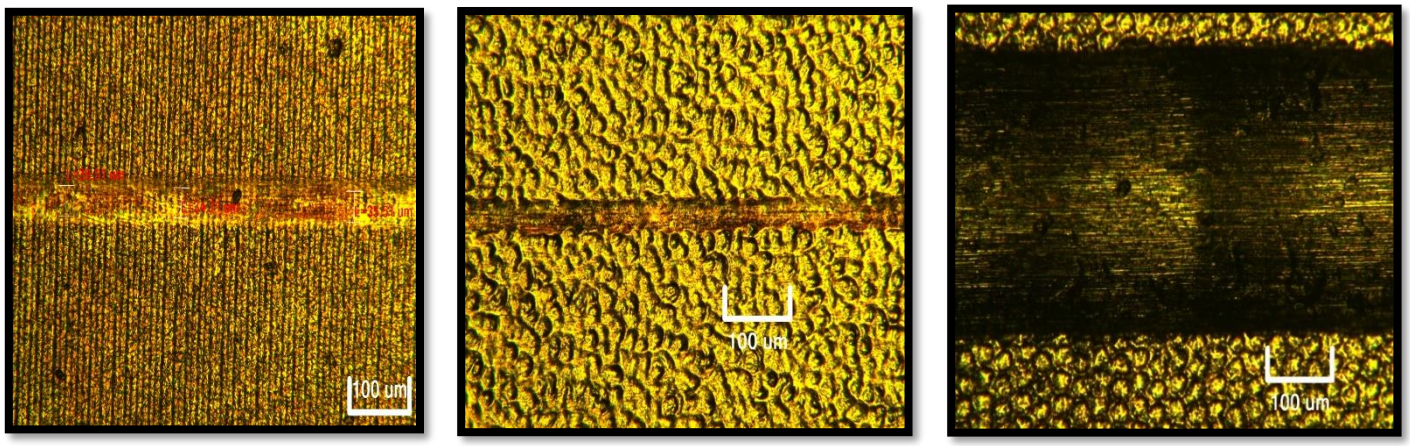

(a) (b) (c)

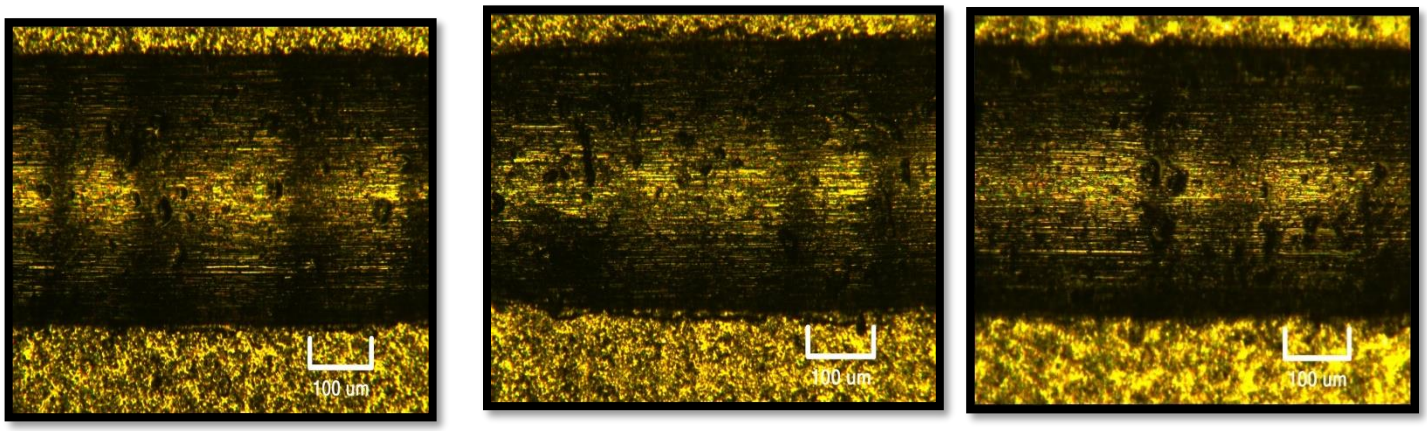

(c) (d) (e)

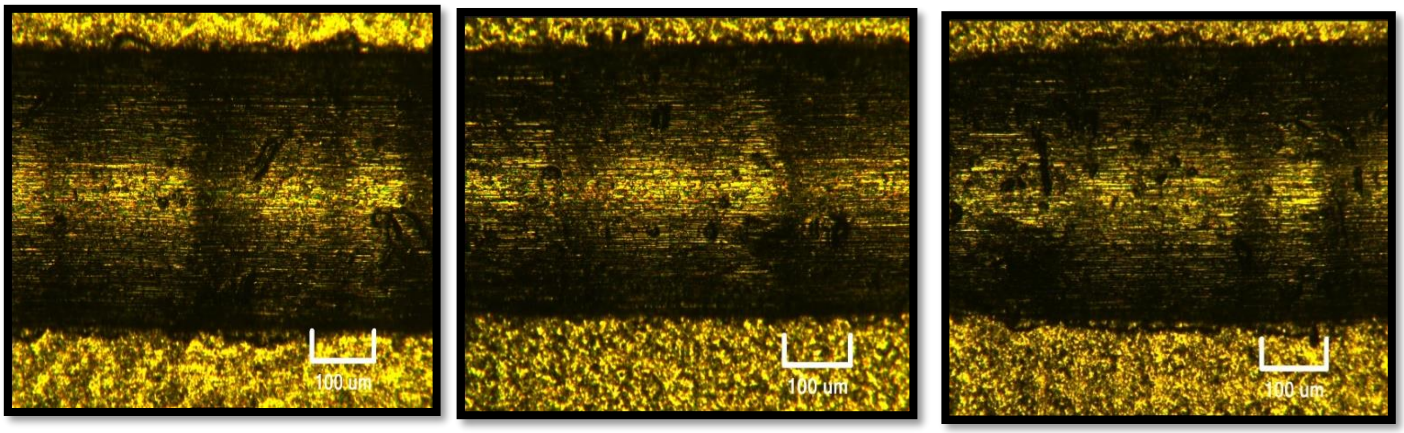

(f) *(g)* *(h)*

Figure 24 : wear track widths for (a) sample1 (b) sample2 (c) sample3 (d) Sample 4 (e) Sample 5 (f)Sample 6 (g) Sample 7 (h) Sample 8 (i) Untextured Sample.

Figure 24 shows the wear track images obtained with an optical microscope for all the samples. Samples with higher dimple densities and laser speed of 400mm/s and 800mm/s (sample 1 and sample 2), show the minimum wear track width, while samples with laser speed ranging from 1200mm/s to 2800mm/s (sample 3 to sample 8), shows almost similar wear tracks with widths less than that of untextured surface. The untextured sample shows the highest wear track width compare to textured surfaces.

The wear tracks were analyzed using NANOVEA ST400 profilometer to obtain the following images.

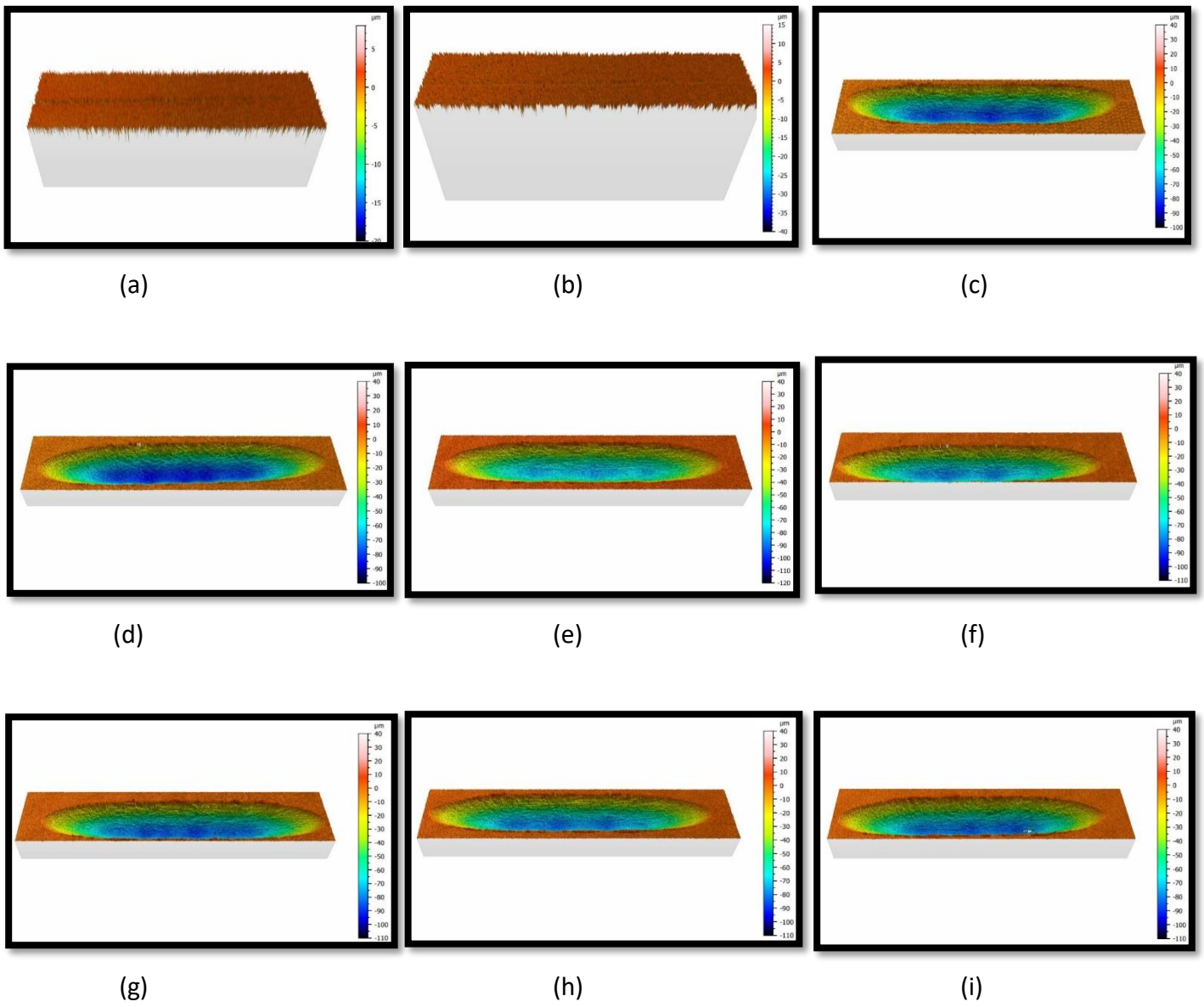

Figure 25: Wear track characterization for (a) sample1 (b) sample2 (c) sample3 (d) Sample 4 (e) Sample 5 (f)Sample 6 (g) Sample 7 (h) Sample 8 (i) Untextured Sample.

Figure 25 shows the wear track characteristics for all the samples. Samples with higher dimple densities and laser speed of 400mm/s and 800mm/s (sample 1 and sample 2), show the smallest

wear tracks while Samples with laser speed ranging from1200mm/s to 2800mm/s (sample 3 to sample 8), shows almost similar wear tracks less than that of untextured surface. The untextured sample has the biggest wear track compare to textured surfaces.

Figure 26 (a) (b) shows the wear track profiles for sample with laser speed 800mm/s (sample 2) and untextured sample. Wear track depth for the sample with highest dimple density is less than 2 microns whereas it is 113.36 microns for an untextured sample.

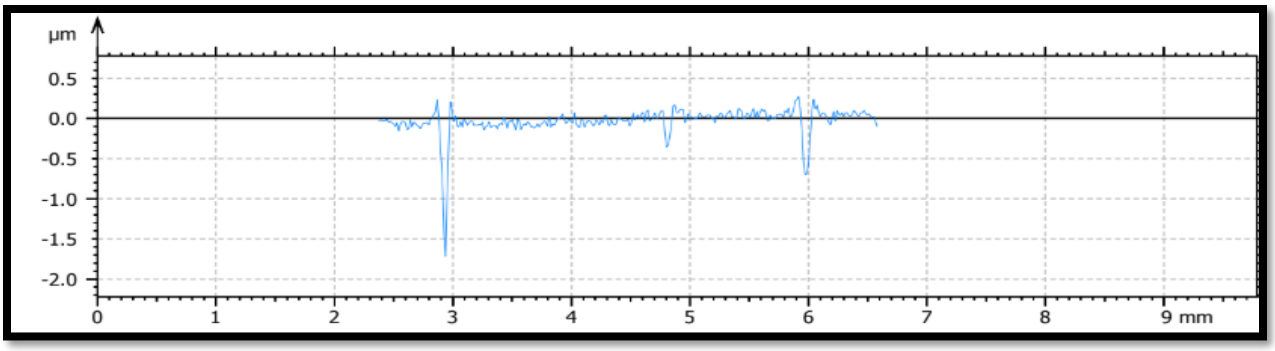

(a)

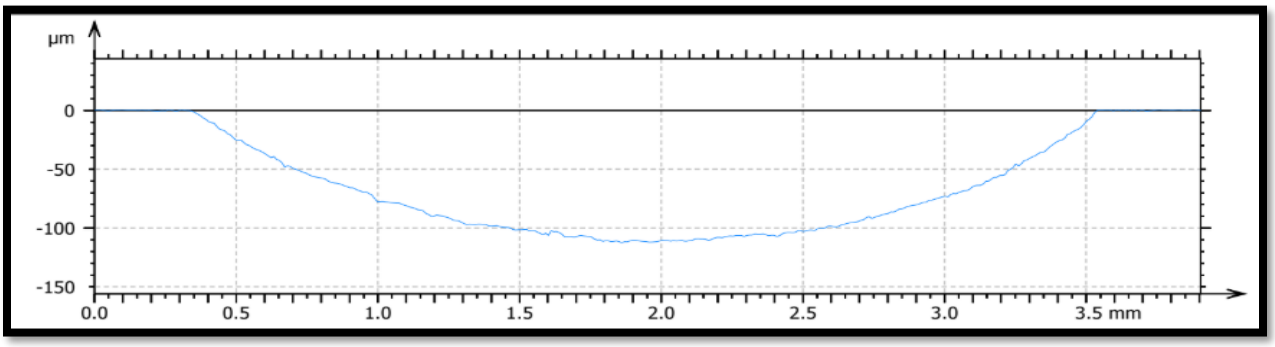

(b)

Figure 26: Wear track profile (a) sample with laser speed 800mm/s (sample 2) and (b) untextured sample.

6.6 Wear Mechanism

To study the wear mechanism, SEM tests were performed on the sample with lower friction and wear and laser speed of 800mm/s (sample 2) and untextured sample.

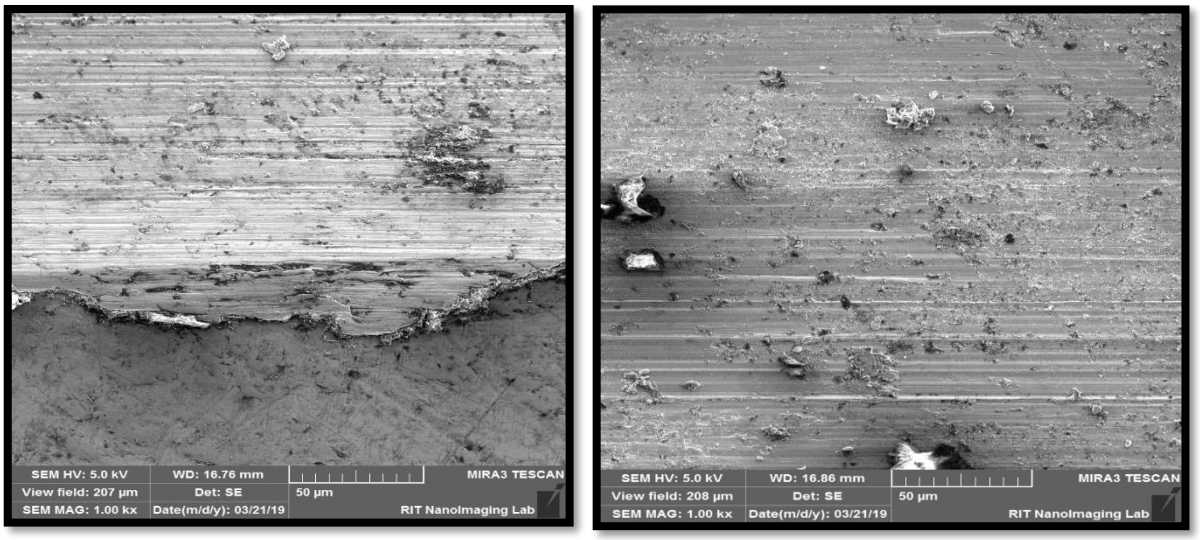

(a) SEM images for untextured sample: (1) edge of wear track (2) enlarged image of wear track

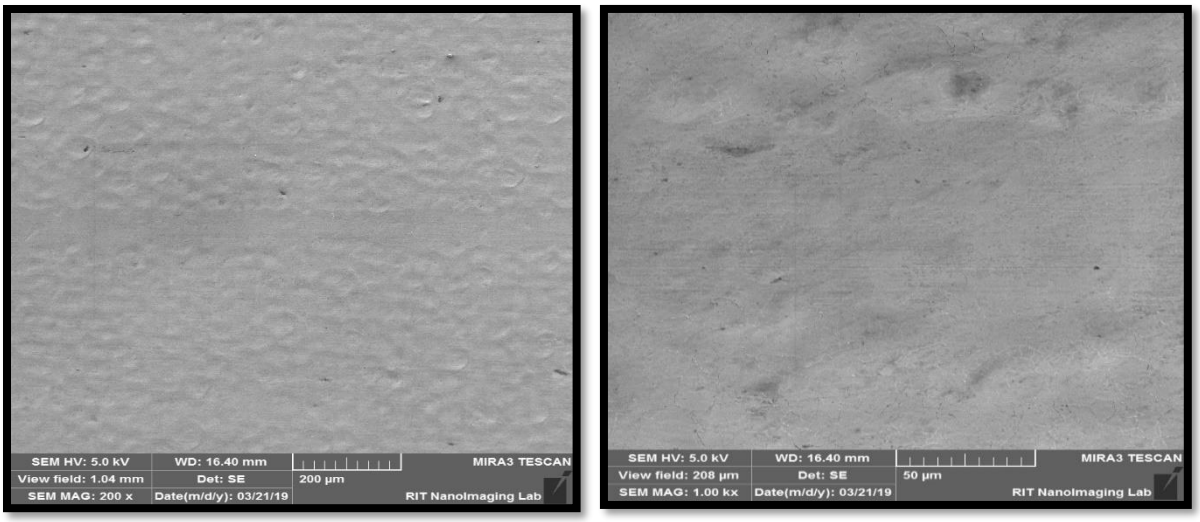

(b) SEM images for Sample with maximum dimple density: (1) wear track (2) Enlarged image of wear track

Figure 27 : SEM images for wear tracks of (a) Untextured sample and (b) sample with maximum dimple density.

Figure 27 shows the SEM images of wear tracks for untextured sample and the sample with laser velocity 800mm/s (sample 2). In untextured sample there is an abrasive wear of the metal surface and permanent deformation at the edge of wear track can be seen in figure 27(a)(1). From figure 27(a)(2) it can be seen that on untextured sample hard particles are ploughed from the metal surface which results in a three-body abrasive wear.

On the other hand, for sample with laser speed of 800mm/s, wear track is very smooth and there is no abrasive wear of metal surface. There is no deformation of material inside wear track and no hard particles can be seen.

6.5 Wearing out of dimples

To validate the wearing out of dimples, tests were performed on sample 3 for 100 seconds and 200 seconds time duration. Figure 28 (a) shows the wear track for a test of 100 seconds and figure 28 (b) shows the wear track for a test of 200 seconds. It is clear that dimples wear out in between 100 seconds and 200 seconds and the graph of friction coefficient jumps at a higher value for sample 3 in this time period.

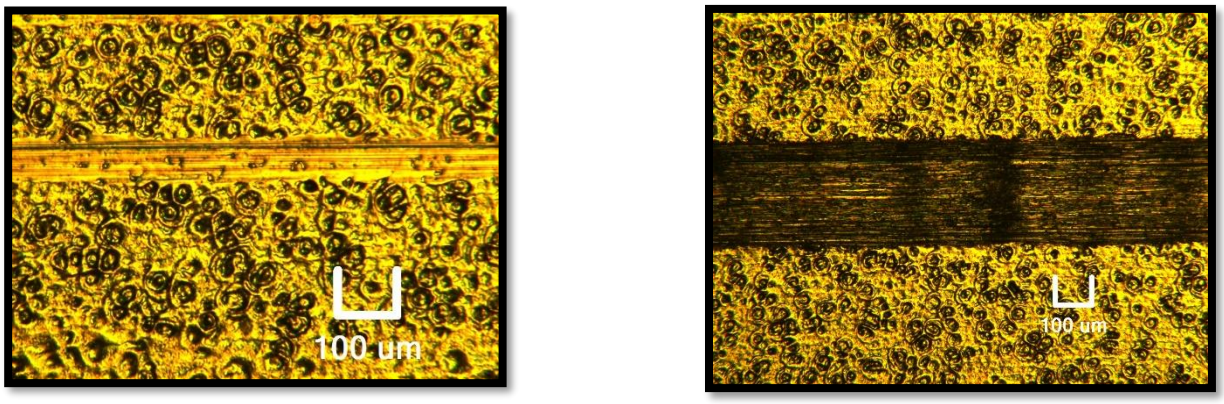

(a) *(b)*

Figure 28 : (a) 100 seconds test, (b) 200 seconds test for sample 3

7.0 CONCLUSION

1. Results showed that laser texturing helps to improve tribological properties of titanium alloy. For all the textured surfaces friction and wear is reduced as compared to untextured sample.
    1.1. Samples with laser speed of 400mm/s and 800mm/s (sample 1 and sample 2), shows friction reduction of around 67% and wear reduction of almost 99%.
    1.2. Sample with laser speed of 400mm/s and dimple density of 50dimples/mm (sample 1), the surface hardness is increased considerably due to longer exposure to laser. This increased surface hardness affect the tribological properties and the friction reduction may not be because of only surface texturing.
    1.3. The second sample with laser speed of 800mm/s and dimple density of 25dimples/mm (sample 2), shows very low increase in surface hardness and it can be said that the reduction in friction is totally due to laser texturing.
    1.4. Samples with laser velocity ranging from 1200mm/s to 2800mm/s (Sample 3 to sample 8), have almost similar friction coefficient which is lower than the untextured sample with average reduction in friction of 6% and in wear 11%.
2. For texturing, change in laser processing velocity caused the change in dimple density on samples. As laser velocity increases, dimple density decreases.
3. Variation in dimple density has very wide effects on the tribological properties of titanium. For samples with laser speed of 400mm/s and 800mm/s (sample 1and sample 2) where dimples overlap each other, friction is reduced drastically. For samples where dimples are not overlapping each other, friction coefficient reduces as dimple density increases.

4. Results showed that sample with laser speed 800mm/s and dimple density of 7.6 dimples/mm (sample 2), gives the best reduction of friction and wear without increasing the surface hardness of titanium.

8.0 FUTURE RESEARCH

Though this research shows great results, there are few areas that could be carried out on forward. These areas are as follows:

1. The effect of varying dimple depth of laser textured surface on tribological properties of titanium can be studied and optimum dimple depth can be found which will give maximum friction and wear reduction.
2. The effect of different textured shapes created by laser texturing can be studied and the best shape which will show higher friction and wear reduction can be found.
3. This research used only PAO as a lubricant but studying the effect of lubricant additives (such as ionic liquids) on the tribological properties of laser textured surface would be really interesting.

9.0 APPENDIX I: Variation of friction Coefficient as a function of time

Following are the friction coefficient graphs for all the samples.

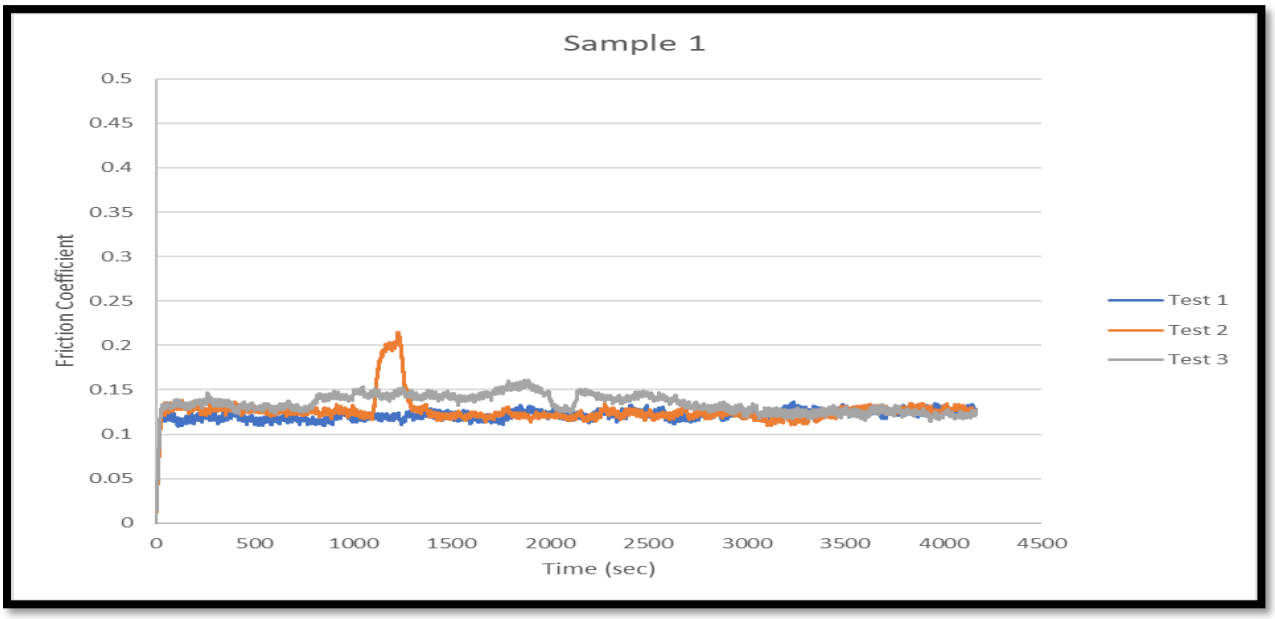

Figure 29 :Variation of friction coefficient for sample 1

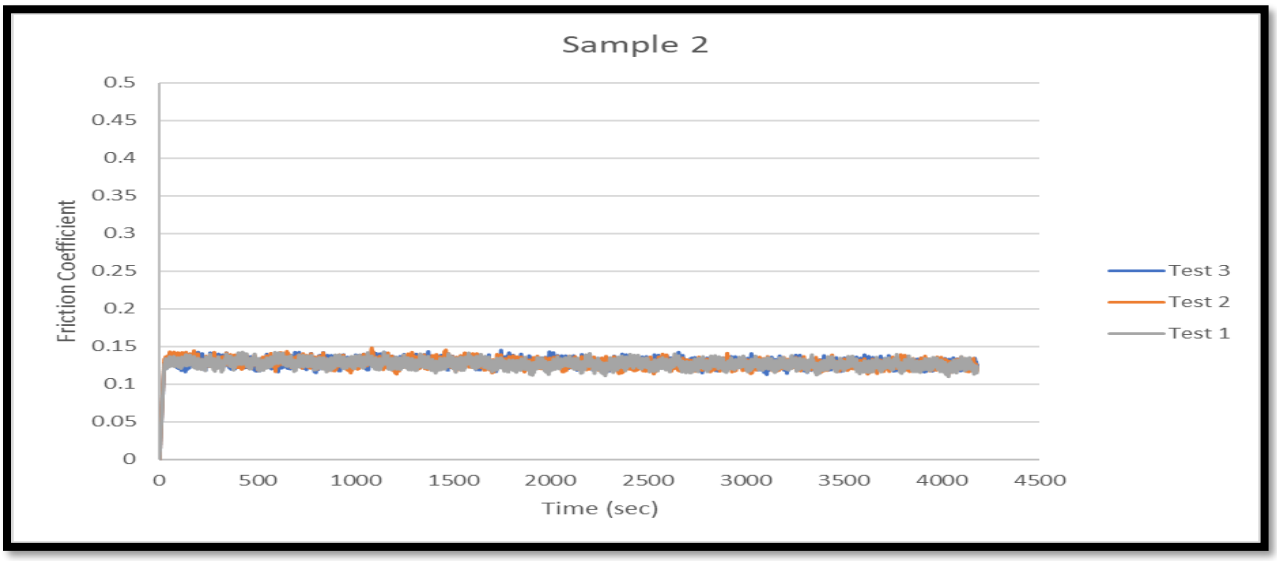

Figure 30 : Variation of friction coefficient for sample 2

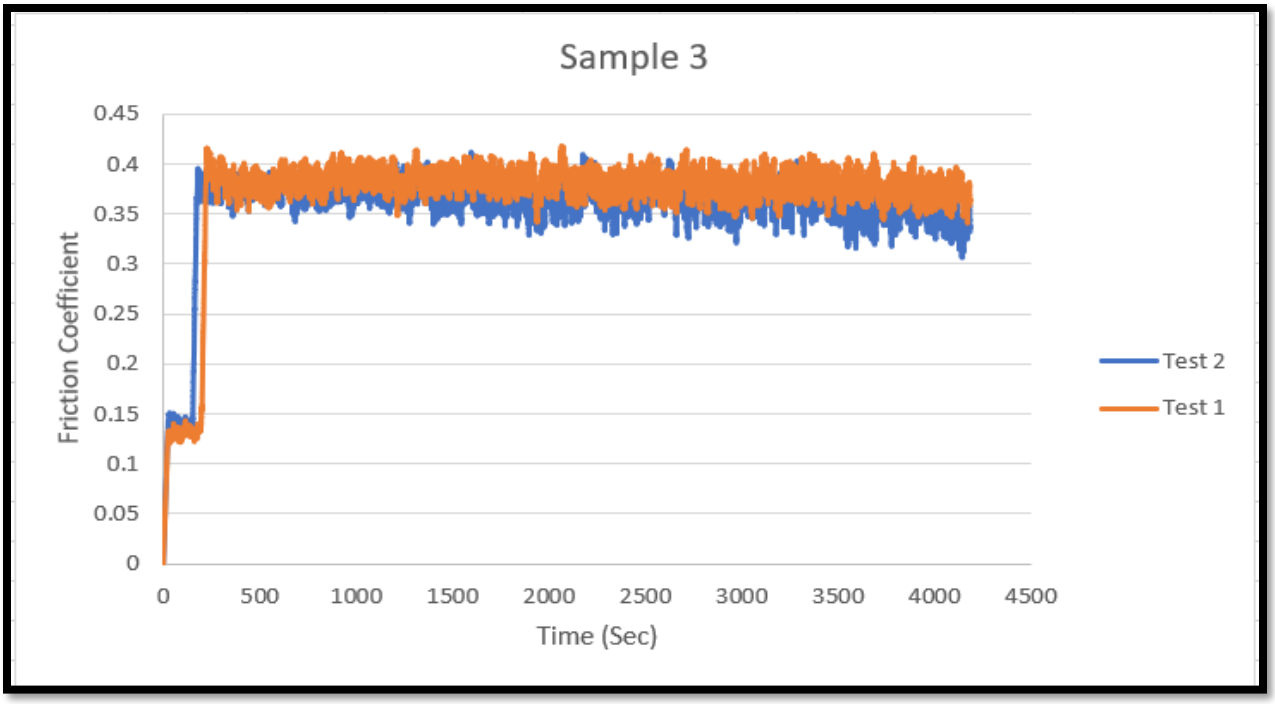

Figure 31 :Variation of friction coefficient for sample 3

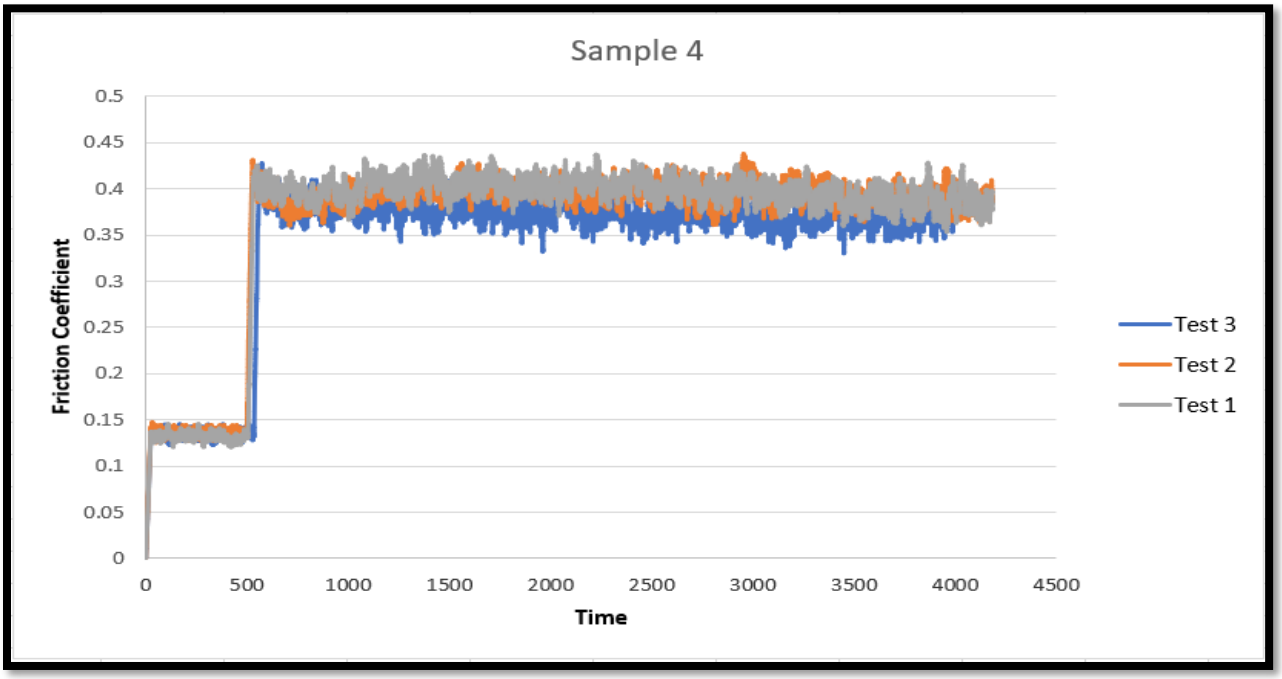

Figure 32 : Variation of friction coefficient for sample 4

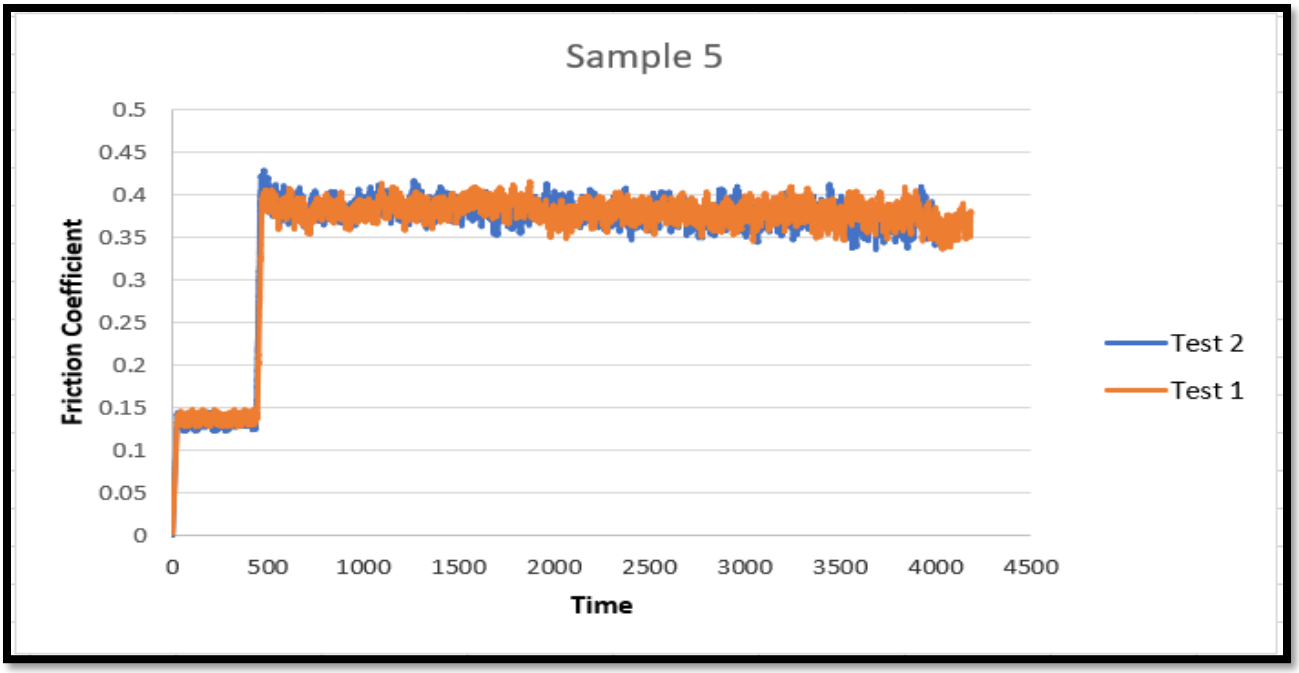

Figure 33 : Variation of friction coefficient for sample 5

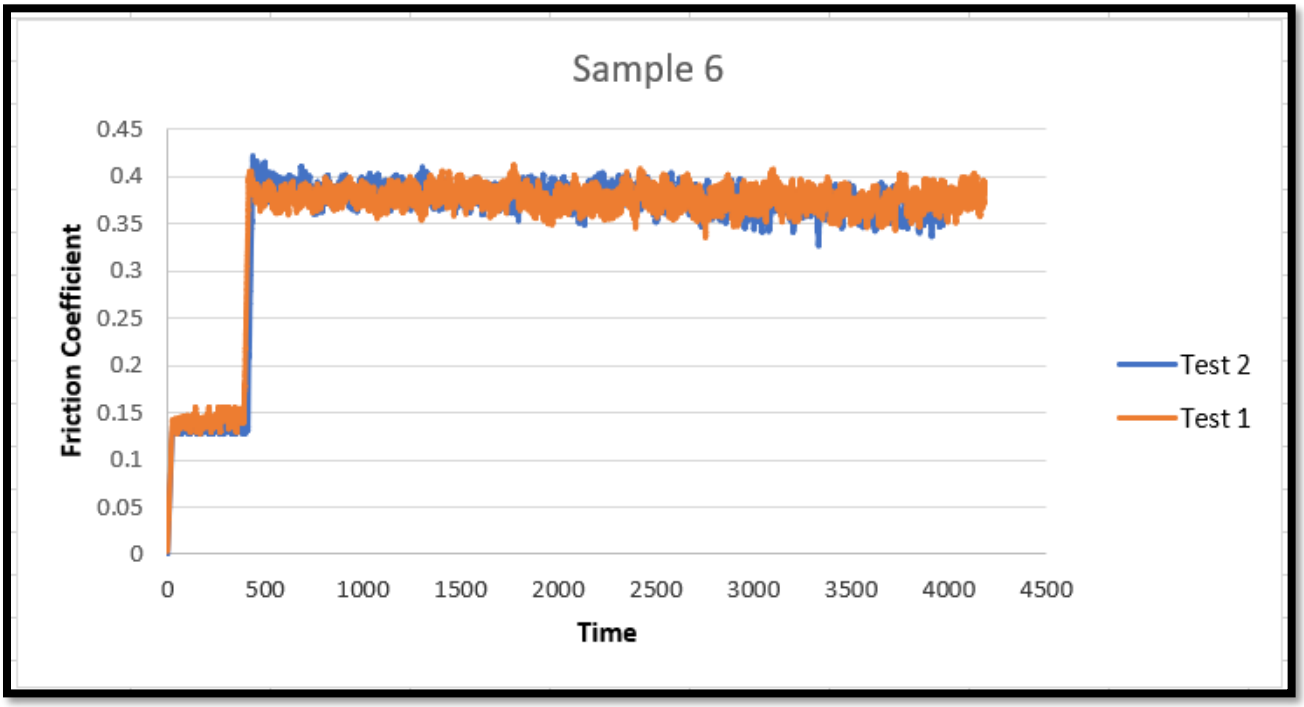

Figure 34 : Variation of friction coefficient for sample 6

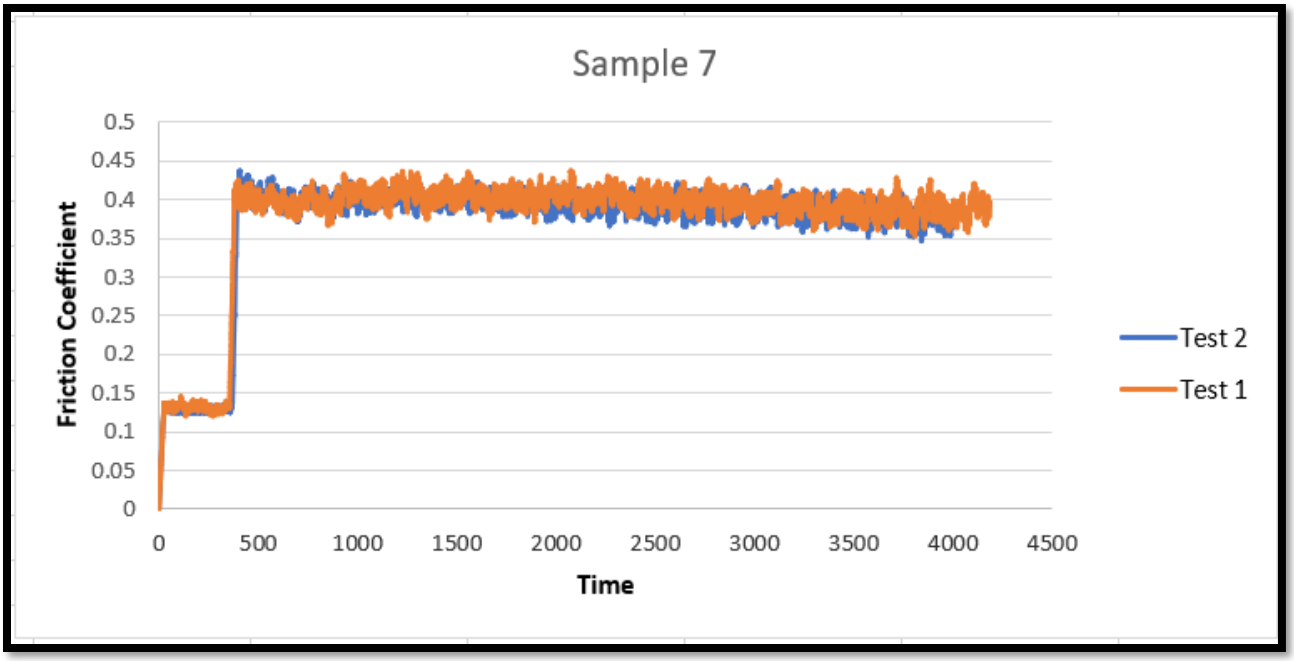

Figure 35 : Variation of friction coefficient for sample 7

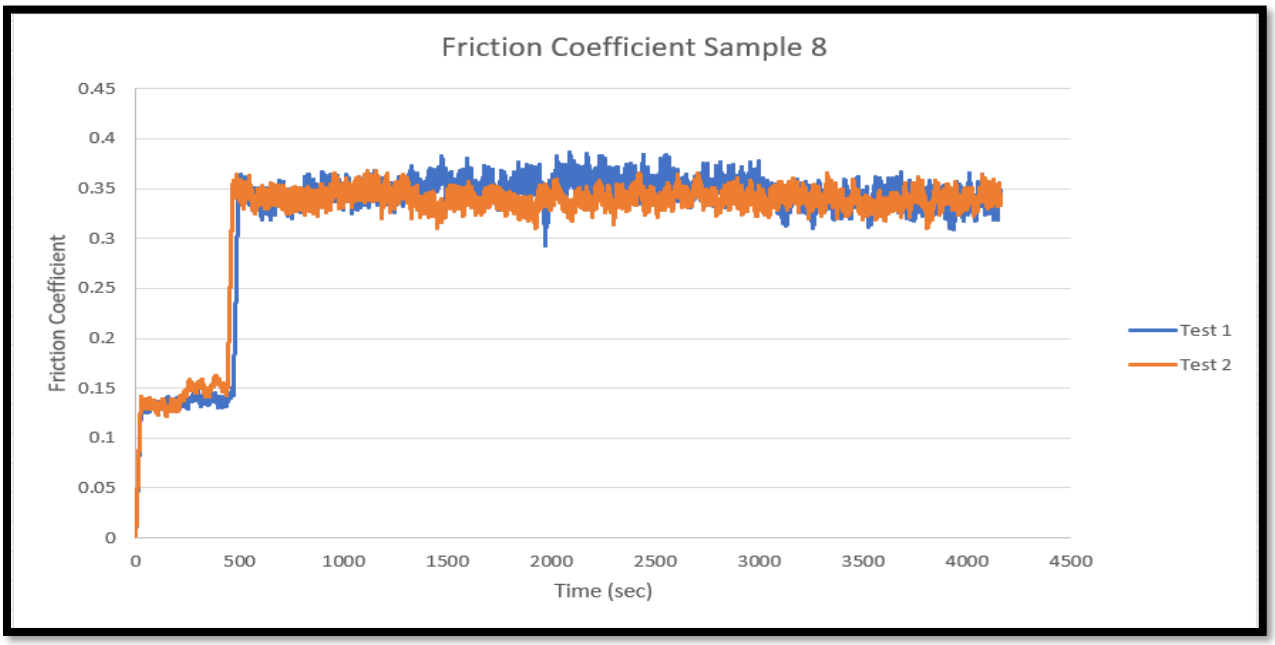

Figure 36 : Variation of friction coefficient for sample 8

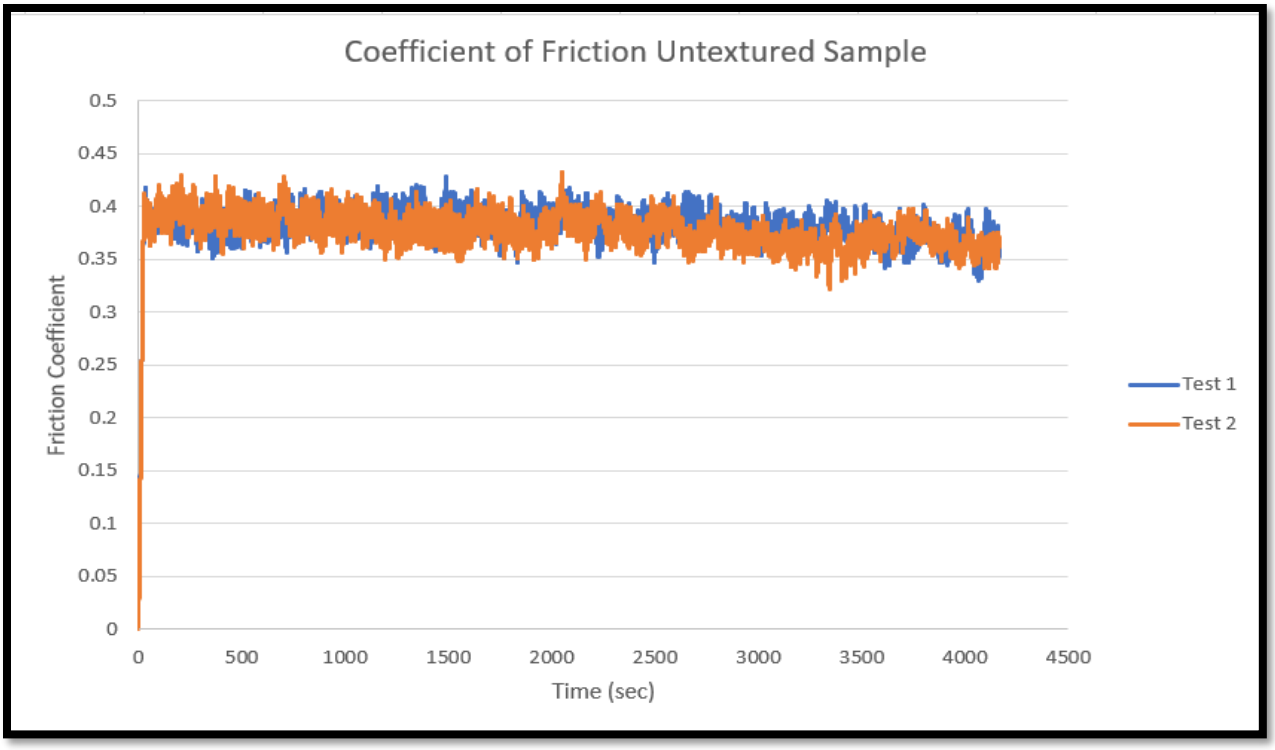

Figure 37 : Variation of friction coefficient for an untextured sample

10.0 APPENDIX II – 3D Images of Samples without wear track.

Following are the 3D images of all the samples.

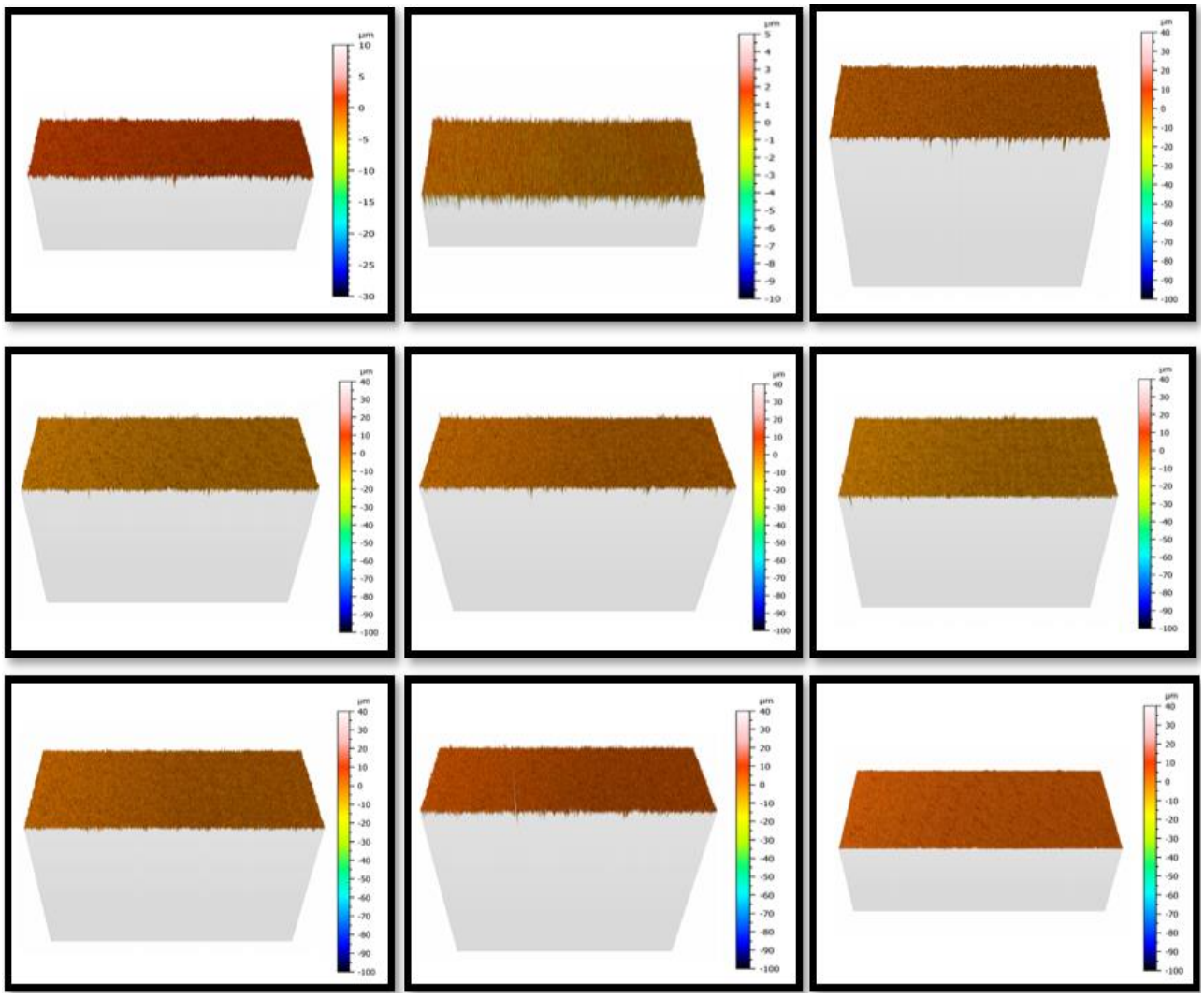

Figure 38: 3D Images of surface characterization for all samples

11.0 REFERENCES

[1] K. Holmberg and A. Erdemir, “Influence of tribology on global energy consumption, costs and emissions,” *Friction*, vol. 5, no. 3, pp. 263–284, 2017.

[2] X. Wang, W. Liu, F. Zhou, and D. Zhu, “Preliminary investigation of the effect of dimple size on friction in line contacts,” *Tribol. Int.*, vol. 42, no. 7, pp. 1118–1123, 2009.

[3] I. Etsion, “State of the Art in Laser Surface Texturing,” *J. Tribol.*, vol. 127, no. 1, p. 248, 2005.

[4] P. Gren, “Feasibility of using digital speckle correlation in the study of seal contacts,” *Lubr. Sci.*, no. April, pp. 123–134, 2009.

[5] K. Li, Z. Yao, Y. Hu, and W. Gu, “Friction and wear performance of laser peen textured surface under starved lubrication,” *Tribol. Int.*, vol. 77, pp. 97–105, 2014.

[6] Wikipedia, “Tribology,” *https://en.wikipedia.org/wiki/Tribology*.

[7] H. Harish, “Study of Stribeck Curve,” *Indian Inst. Technol. Delhi*.

[8] H. Zhang, H. Chen, X. Shi, X. Liu, and G. Duan, “Tribological properties of ionic liquids for steel/aluminum, steel/copper and steel/Si_3N_4 ceramic contacts under boundary lubrication,” *Ind. Lubr. Tribol.*, vol. 70, no. 7, pp. 1158–1168, 2018.

[9] B. M., “Boundary Lubrication.”

[10] International Energy Agency, *Energy Technology Perspectives: Scenarios & Strategies To 2050*. 2010.

[11] K. Holmberg, R. Siilasto, T. Laitinen, P. Andersson, and A. Jäsberg, “Global energy consumption due to friction in paper machines,” *Tribol. Int.*, vol. 62, pp. 58–77, 2013.

[12] K. Holmberg, P. Kivikytö-Reponen, P. Härkisaari, K. Valtonen, and A. Erdemir, “Global energy consumption due to friction and wear in the mining industry,” *Tribol. Int.*, vol. 115, no. February, pp. 116–139, 2017.

[13] K. Holmberg, P. Andersson, and A. Erdemir, “Global energy consumption due to friction in passenger cars,” *Tribol. Int.*, vol. 47, pp. 221–234, 2012.

[14] Wikipedia, “https://en.wikipedia.org/wiki/ Mode_of_transport,” *Mode Transp.*

[15] W. Dai, B. Kheireddin, H. Gao, and H. Liang, “Roles of nanoparticles in oil lubrication,” *Tribol. Int.*, vol. 102, pp. 88–98, 2016.

[16] A. Hirata, “Nanolubricants and applications -nanotechnology in solid lubrication,” *IECON Proc. (Industrial Electron. Conf.*, vol. 2005, pp. 2386–2388, 2005.

[17] A. Erdemir *et al.*, “Carbon-based tribofilms from lubricating oils,” *Nature*, vol. 536, no. 7614, pp. 67–71, 2016.

[18] F. J. C. P.Iglesias, MD.Bermúdez, “Friction and wear of aluminium–steel contacts lubricated with ordered fluids-neutral and ionic liquid crystals as oil additives,” 2004.

[19] B. Tormos, L. Ramírez, J. Johansson, M. Björling, and R. Larsson, “Fuel consumption and friction benefits of low viscosity engine oils for heavy duty applications,” *Tribol. Int.*, vol. 110, no. February, pp. 23–34, 2017.

[20] A. Singh, S., Singh, S., and Sehgal, “Impact of Low Viscosity Engine Oil on Performance, Fuel Economy and Emissions of Light Duty Diesel Engine," SAE Technical Paper 2016-01-2316, 2016.”

[21] Z. et al. Cuthbert, J., Gangopadhyay, A., Elie, L., Liu, “Engine Friction and Wear Performances with Polyalkylene Glycol Engine Oils," SAE Technical Paper 2016-01-2271, 2016.”

[22] A.E.JiménezM.D.BermúdezP.IglesiasF.J.CarriónG.Martínez-Nicolás, “1-N-alkyl -3-methylimidazolium ionic liquids as neat lubricants and lubricant additives in steel–aluminium contacts,” 2006.

[23] N. Argibay, J. H. Keith, B. A. Krick, D. W. Hahn, G. R. Bourne, and W. G. Sawyer, “High-temperature vapor phase lubrication using carbonaceous gases,” *Tribol. Lett.*, vol. 40, no. 1, pp. 3–9, 2010.

[24] C. Greiner, J. R. Felts, Z. Dai, W. P. King, and R. W. Carpick, “Controlling Nanoscale Friction through the Competition between Capillary Adsorption and Thermally Activated Sliding,” *ACS Nano*, vol. 6, no. 5, pp. 4305–4313, May 2012.

[25] P. I. Sameer Magar, Hong Guo, “Estimation of Energy Conservation in Internal Combustion Engine Vehicles Using Ionic Liquid As an Additive,” *Int. Mech. Eng. Congr. Expo.*, pp. 1–6, 2019.

[26] A. John and P. I. Keil Steven, Hong Gou, “The Effects of Single-Walled Carbon Nanotubes and Ionic Liquids in Reduction of Friction and Wear,” *Int. Mech. Eng. Congr. Expo.*, 2019.

[27] K. M. Nadano Hiromasa, Nakasako Masakazu, “1 . Effect of Anti-Wear Additives on Seizure Resistance of Vegetable Oils in Four-Ball Test,” *Japan Soc. Mech. Eng.*, no. 1, p. 2019, 2004.

[28] S. Bagherifard, I. Fernandez-Pariente, R. Ghelichi, and M. Guagliano, “Severe Shot Peening to Obtain Nanostructured Surfaces: Process and Properties of the Treated Surfaces,” *Handbook of Mechanical Nanostructuring*. 24-Jul-2015.

[29] M. A. Holmberg K, “Coatings Tribology–Properties, Mechanisms, Techniques and Applications in Surface Engineering. Elsevier Tribology and Interface Engineering Elsevier Series. Amsterdam, the Netherlands: Elsevier; 2009.”

[30] S. Venkatesan, “Surface textures for enhanced lubrication : Fabrication and characterization techniques,” *Proc. World Tribol. Congr. III - 2005,* p. 40506, 2005.

[31] A. de Kraker, R. A. J. van Ostayen, A. van Beek, and D. J. Rixen, “A Multiscale Method Modeling Surface Texture Effects,” *J. Tribol.*, vol. 129, no. 2, p. 221, 2007.

[32] E. Gualtieri, A. Borghi, L. Calabri, N. Pugno, and S. Valeri, “Increasing nanohardness and reducing friction of nitride steel by laser surface texturing,” *Tribol. Int.*, vol. 42, no. 5, pp. 699–705, 2009.

[33] A. Kovalchenko, O. Ajayi, A. Erdemir, G. Fenske, and I. Etsion, “The Effect of Laser Texturing of Steel Surfaces and Speed-Load Parameters on the Transition of Lubrication Regime from Boundary to Hydrodynamic,” *Tribol. Trans.*, vol. 47, no. 2, pp. 299–307, Apr. 2004.

[34] R. Gandhi, D. Sebastian, S. Basu, J. B. Mann, P. Iglesias, and C. Saldana, “Surfaces by vibration/modulation-assisted texturing for tribological applications,” *Int. J. Adv. Manuf. Technol.*, vol. 85, no. 1–4, pp. 909–920, 2016.

[35] D. Braun, C. Greiner, J. Schneider, and P. Gumbsch, “Efficiency of laser surface texturing in the reduction of friction under mixed lubrication,” *Tribol. Int.*, vol. 77, pp. 142–147, 2014.

[36] P. Mehta, R. Liu, J. B. Mann, C. Saldana, and P. Iglesias, “Effect of textured surfaces created by modulation-assisted machining on the Stribeck curve and wear properties of steel-aluminum contact,” *Int. J. Adv. Manuf. Technol.*, vol. 99, no. 1, pp. 399–409, 2018.

[37] E. De La Guerra Ochoa *et al.*, “Optimising lubricated friction coefficient by surface texturing,” *Proc. Inst. Mech. Eng. Part C J. Mech. Eng. Sci.*, vol. 227, no. 11, pp. 2610–2619, 2013.

[38] P. Mehta, “Tribological Study of Textured Surfaces created using Modulation Assisted Machining for Steel- Aluminum Contact,” 2016.

[39] H. Yu, X. Wang, and F. Zhou, “Geometric shape effects of surface texture on the generation of hydrodynamic pressure between conformal contacting surfaces,” *Tribol. Lett.*, vol. 37, no. 2, pp. 123–130, 2010.

[40] H. L. Costa and I. M. Hutchings, “Some innovative surface texturing techniques for tribological purposes,” *Proc. Inst. Mech. Eng. Part J J. Eng. Tribol.*, vol. 229, no. 4, pp. 429–448, Jun. 2014.

[41] E. Gualteri, "'Improving tribological properties of steels by surface texturing and coating,' p. 100.," 2008.

[42] M. A. Iturralde, "'Surface Micro Texturing Using Modulation assisted Machining,' The Pennsylvania State University.," 2013.

[43] S. Matsumura, T., and Takahashi, "'Micro dimple milling on cylinder surfaces,' J. Manuf. Process., 14(2), pp. 135–140.," 2012.

[44] Y. G. Schneider, "'Formation of surfaces with uniform micropatterns on precision machine and instruments parts,' Precis. Eng., 6(4), pp. 219–225.," 1984.

[45] C. Greco, A., Raphaelson, S., Ehmann, K., Wang, Q. J., and Lin, "'Surface Texturing of Tribological Interfaces Using the Vibromechanical Texturing Method,' J. Manuf. Sci. Eng., 131(6), p. 61005.," 2009.

[46] J. Salguero, I. Del Sol, J. M. Vazquez-martinez, M. J. Schertzer, and P. Iglesias, "Effect of laser parameters on the tribological behavior of Ti6Al4V titanium microtextures under lubricated conditions," *Wear*, vol. 426–427, no. December 2018, pp. 1272–1279, 2019.

[47] P.AnderssonaJ.KoskinenaS.VarjusaY.GerbigbH.HaefkebS.GeorgioucB.Zhmudd1W.Busse, "Microlubrication effect by laser-textured steel surfaces," 2007.

[48] M. Pang, X. Liu, and K. Liu, "Effect of wettability on the friction of a laser-textured cemented carbide surface in dilute cutting fluid," *Adv. Mech. Eng.*, vol. 9, no. 12, pp. 1–9, 2017.

[49] J. Qu and J. J. Truhan, "An efficient method for accurately determining wear volumes of

sliders with non-flat wear scars and compound curvatures," *Wear*, vol. 261, no. 7–8, pp. 848–855, 2006.